

“ ” 20 . .

( )

151 « “ ” ’ - »

:

---

---

:

---

:

---

:

---

«

»

---

«

»:

---

151 « \_\_\_\_\_ , \_\_\_\_\_ - \_\_\_\_\_ »

« \_\_\_\_\_ » \_\_\_\_\_ 20\_\_ .

1.

\_\_\_\_\_

\_\_\_\_\_

15.09.2023 1810/ .

2.

: 02.10.23 31.12.23

3.

4.

:

\_\_\_\_\_ ,

\_\_\_\_\_ , \_\_\_\_\_

\_\_\_\_\_ , \_\_\_\_\_ , \_\_\_\_\_

5.

:

\_\_\_\_\_ , \_\_\_\_\_ , \_\_\_\_\_ **PowerPoint.**

6.

-

/			
---	--	--	--

1		1.09-15.09	
2		18.09-2.10	
3		3.10-16.10	
4	2	17.10-25.10	
5		25.10-14.11	
6	3	15.11-28.11	
7	.	28.11-15.12	

7.


8. : 02.10 “ 2023 .”

\_\_\_\_\_ . . .  
 ( ) ( . . . )

\_\_\_\_\_ . . .  
 ( ) ( . . . )

«

»

: 103 ., 54 ., 3

. 103

,

—

.

.

—

.

—

.

—

,

,

,

.

,

.

,

.

:

,

,

,

.

.....	7
1.	9
1.1.	9
1.1.1	9
1.1.2.	11
1.1.3.	13
1.1.4.	14
1.2.	( )..... 16
1.2.1.	17
1.2.2.	21
1.2.3.	26
1.2.4.	33
2.	41
2.1.	41
2.1.1.	41
2.1.2.	42
2.1.3.	43
2.1.4.	VCG ..... 45
2.1.5.	, ..... 48
2.1.6.	..... 49
2.1.7.	..... 51
2.2.	..... 54
2.2.1.	..... 54
2.2.2.	ARMA ..... 55
2.2.3.	- ..... 58
(MALLAT).....	58
2.2.4.	- ..... 59
2.2.5.	..... 60
2.3.	..... 65
2.3.1.	, ..... 65

2.3.2.	.....	68
2.3.3.	.....	70
2.3.4.	.....	71
3.		77
3.1.	.....	78
3.2.	.....	81
4.	.....	87
4.1.	.....	87
4.2.	.....	88
4.3.	.....	96
	.....	103
	.....	104

17

18

20-

[2]. 1960-

[3].

[4].

(IMU) [5],

[6]. IMU

[7],

[8].

:  
- ;  
- ;  
- ,  
; ;  
- ;  
- ;  
- ;  
.



1.1.

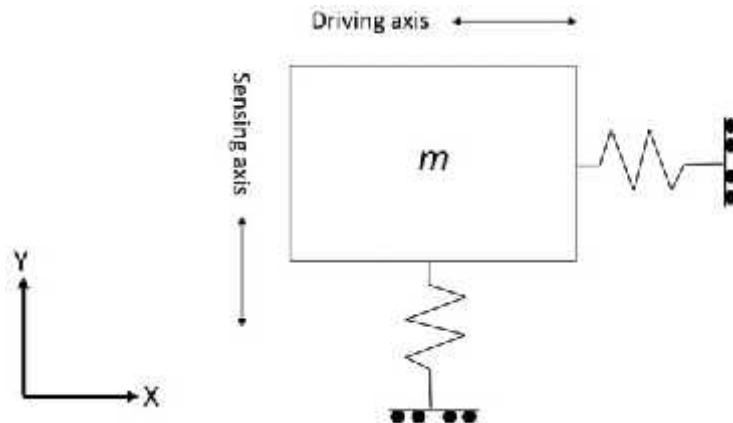
: — , — ,

1.1.1

« *m* »

[12].

.1.1.



1.1.

:

$$m \frac{d^2x}{dt^2} + c \frac{dx}{dt} + kx = F_D + 2m \frac{dx}{dt} \quad \#(1.1)$$

$$2m \frac{dx}{dt}$$

(1.1)

$$m \frac{d^2x}{dt^2} + c \frac{dx}{dt} + kx = F_D \quad \#(1.2)$$

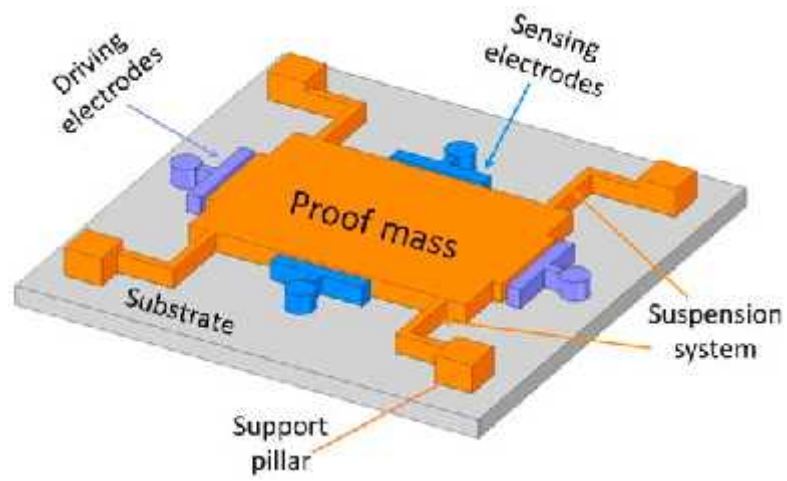
$$m \frac{d^2y}{dt^2} + c \frac{dy}{dt} + ky = F_S - F_C \quad \#(1.3)$$

$$F_C = -2m \frac{dy}{dt} \quad \#(1.4)$$

$F_D, F_S, F_C$  - , ,  $m$  -  
 ,  $x$  - ,  $y$  - ,  
 ,  $c$  - ,  $k$  - -

1.2.,

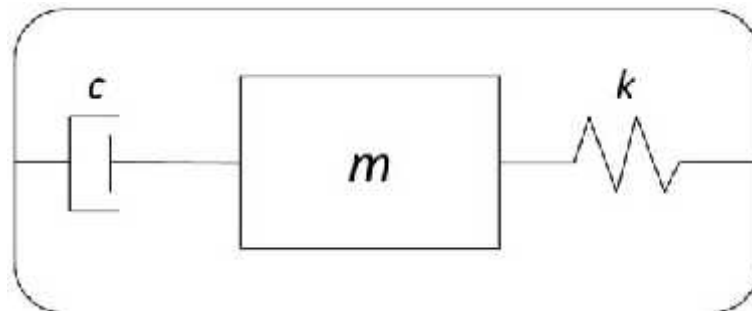
[13].



1.2.

1.1.2.

.1.3.



1.3.

$$m \frac{d^2x}{dt^2} + c \frac{dx}{dt} + kx = F \quad \#(1.5)$$

$$\zeta = \frac{c}{c_c} = \frac{c}{2\sqrt{km}} \quad \#(1.6)$$

$$\omega_n = \sqrt{\frac{k}{m}} \quad \#(1.7)$$

$m$  – ,  $c$  – ,  $k$  –  
,  $c_c$  – ,  $n$  – , –  
.

$$\frac{d^2x}{dt^2} + 2\omega_n\zeta \frac{d}{d} + \omega_n^2 x = \frac{F}{m} \#(1.8)$$

$$m_D \frac{d^2x}{dt^2} + c_D \frac{d}{d} + k_D x = F_D \sin \omega \#(1.9)$$

$m_D$  – ,  $c_D$  – ,  $k_D$  –

$$F = F_0 \sin \omega .$$

$Q_D$   $D$

(1.10).

$$x = x_0 \sin(\omega + \varphi) \#(1.10)$$

$$x_0 = \frac{F_0}{k \sqrt{\left(1 - \left(\frac{\omega}{\omega_D}\right)^2\right)^2 + \left(\frac{\omega}{Q_D \omega_D}\right)^2}} \#(1.11)$$

$$\omega_D = \sqrt{\frac{k_D}{m_D}} \#(1.12)$$

$$Q_D = \frac{m_D \omega_D}{c_D} \#(1.13)$$

(1.14).

$$x_0 = \frac{Q_D F_D}{m_D \omega_D^2} \#(1.14)$$

1.1.3.

$F_C$

(1.4).

C

$x_0$ .

$$x = x_0 \sin(\omega t + \varphi).$$

$$F_C = -2m_C \Omega x_0 \omega_D \cos(\omega_D t + \varphi_D) \#(1.15)$$

$$m_S \frac{d^2 y}{dt^2} + c_S \frac{d}{d} + k_S y = -2m_C x_0 \omega_D \Omega \cos(\omega_D t + \varphi_D) \#(1.16)$$

$Q_S$

S

$$y_0 = \left( \frac{\Omega m_c \omega_D}{m_s \omega_s^2} \right) \frac{F_0}{k \sqrt{\left(1 - \left(\frac{\omega_D}{\omega_s}\right)^2\right)^2 + \left(\frac{\omega}{Q_s \omega_s}\right)^2}} \#(1.17)$$

$$\omega_s = \sqrt{\frac{k_s}{m_s}} \#(1.18)$$

$$Q_s = \frac{m_s \omega_s}{c_s} \#(1.19)$$

—  
.  
, (1.20).

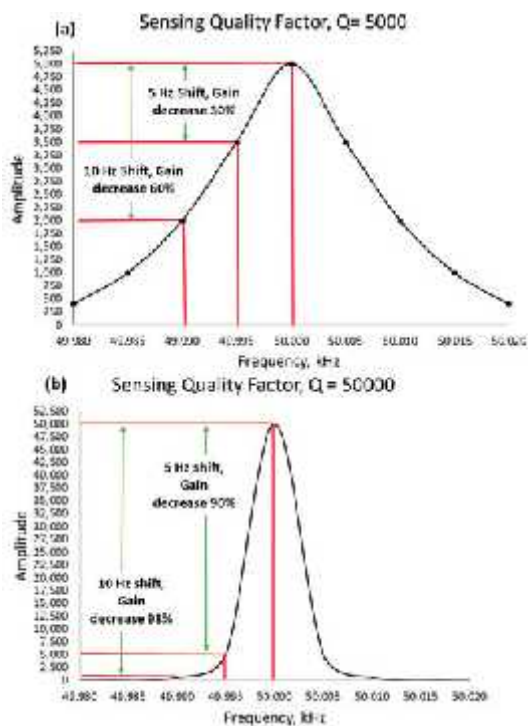
$$y_0 = \frac{2\Omega m_c Q_s x_0}{m_s \omega_s} \#(1.20)$$

- :
1.  $x_0$ .
  2.  $m_c$
- $m_s$ .
3. ,
- $Q_s$ .

#### 1.1.4.

[15,16,17].

.1.4, 50, 50 000, 90%, 5000, 30%, 5



4.1.

(a)

(b)

[18,19].

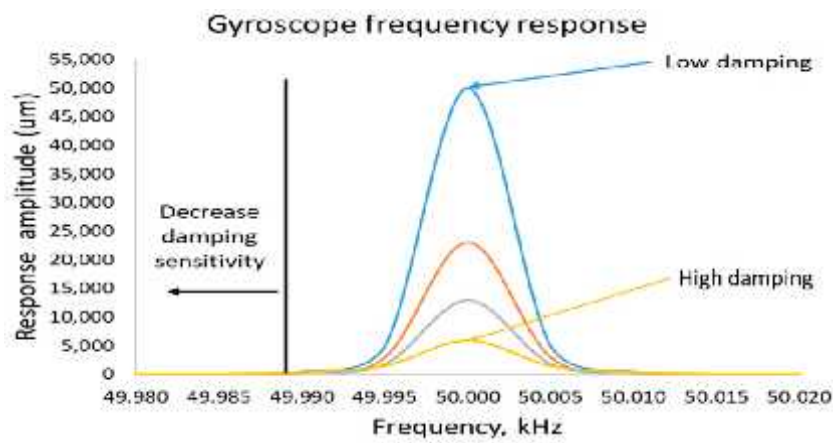
[20].

(1.21).

$$\Delta f = f_S - f_D = \frac{1}{2\pi}(\omega_S - \omega_D) \quad (1.21)$$

$f_S - f_D -$

$Q_S$



1.5.

1.2.

( )

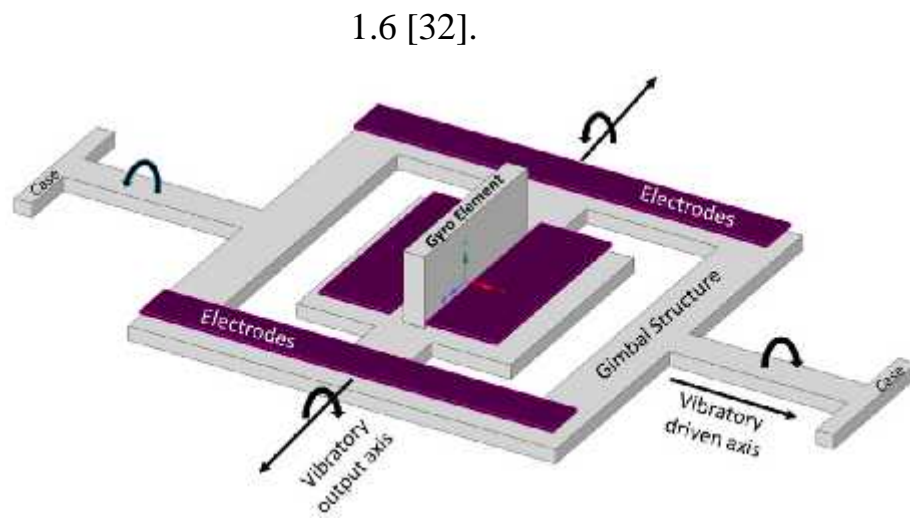
(IC)

[21].





350 × 500



1.6.

Draper

1996

Draper

(VVOG).

1

Pyrex.

60 [33]

Draper [34].

[35].

(ARW)

0,14 / ,

65 / .

z

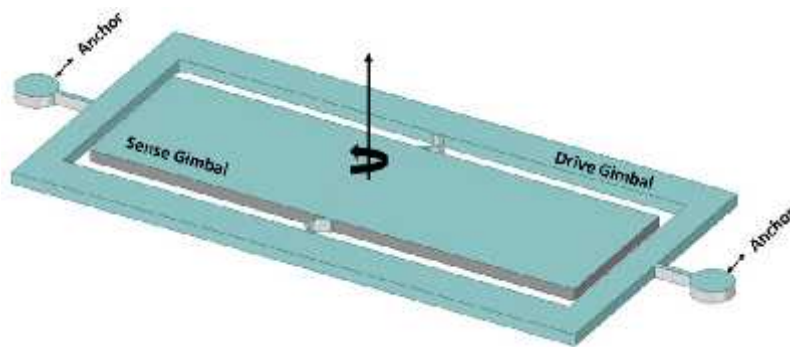
[36].

UV-LIGA Ni-Fe, SU-8 [37].

8

70% Ni, 15% Fe 10% Ni-Fe C, MEM

Ni-Fe 1.7.

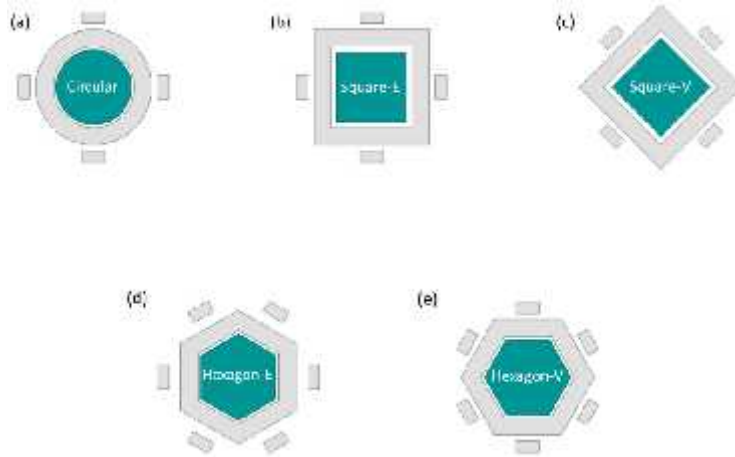


1.7.

Ni-Fe.

[38].

.1.8.



1.8.

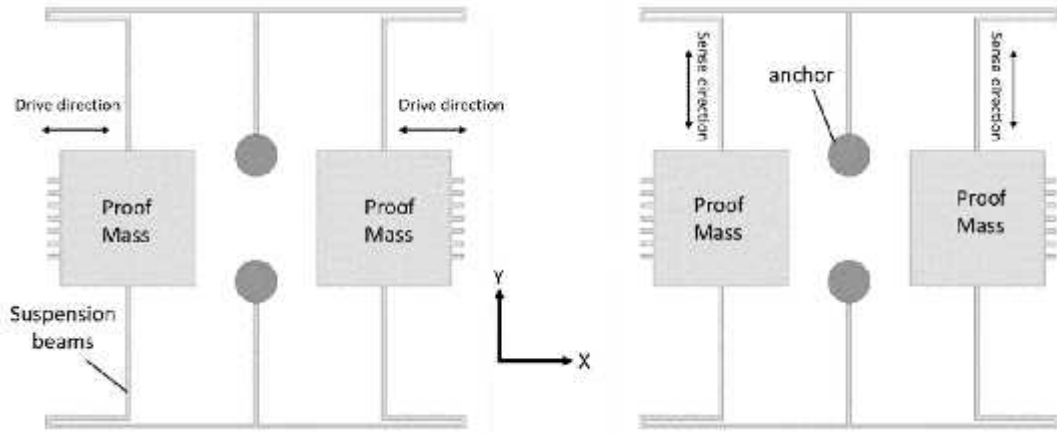
(a) (b) (c)  
(d) (e)

1.2.2.

[39].

[40].

1.9.



1.9.

1993

.

1 ,

100 / .

;

6 ,

,

,

,

,

,

90 / / .

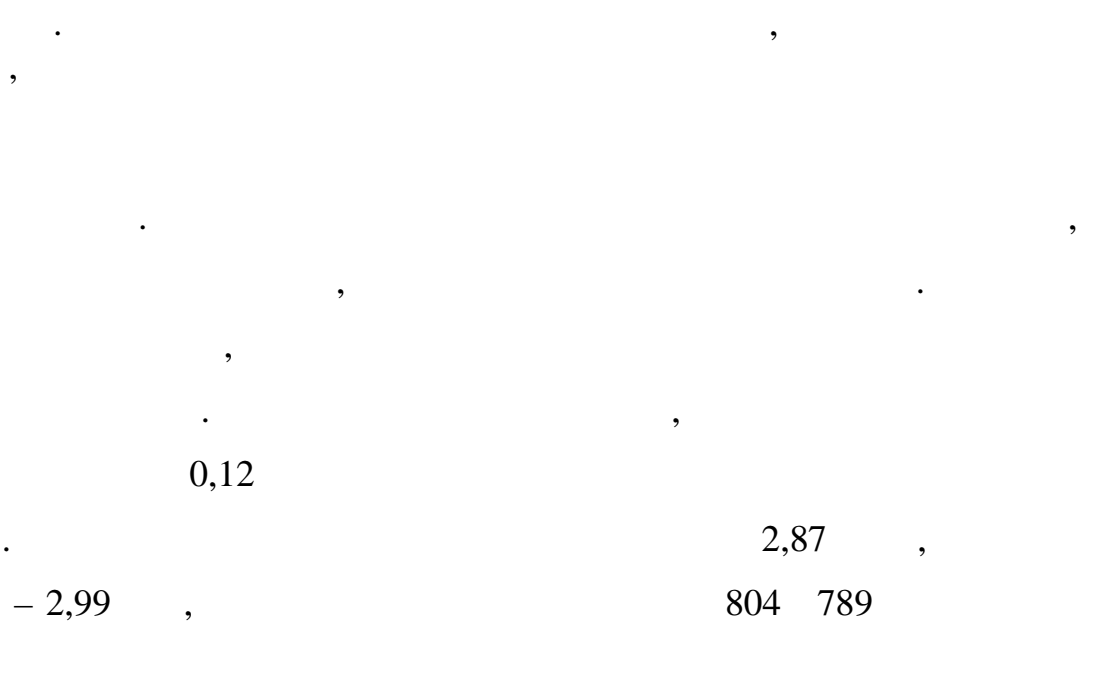
0,1

/ ,

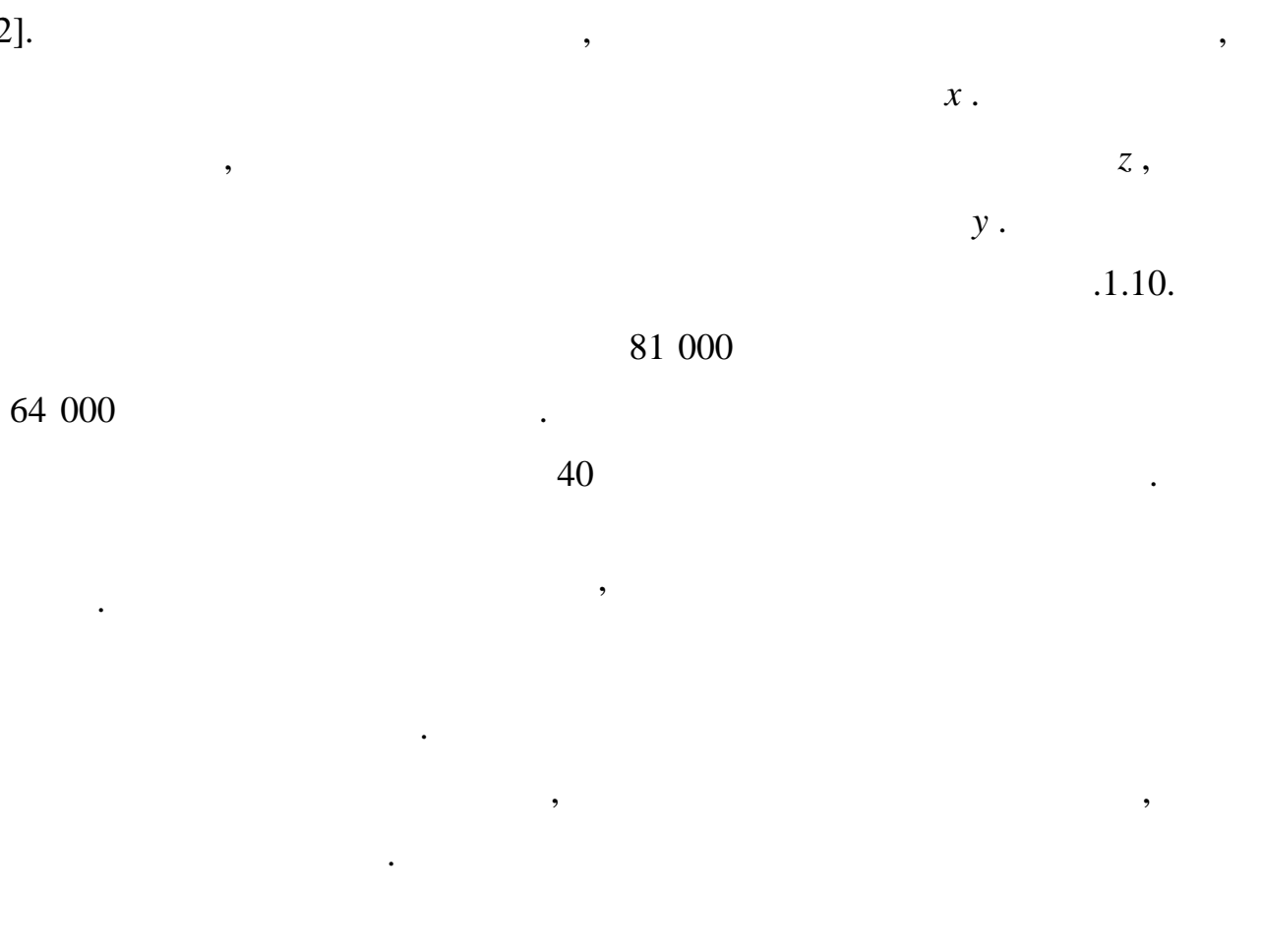
0,2 /

1 .

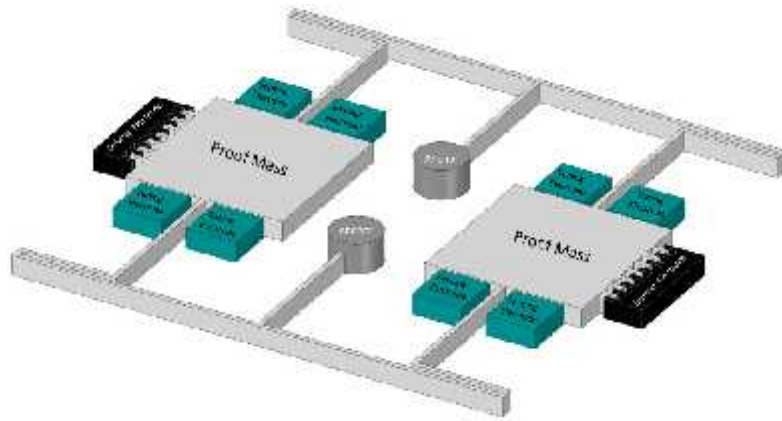
(DRIE) [41].



[42].



1,25 / / .



1.10.

Nguyen

Z,

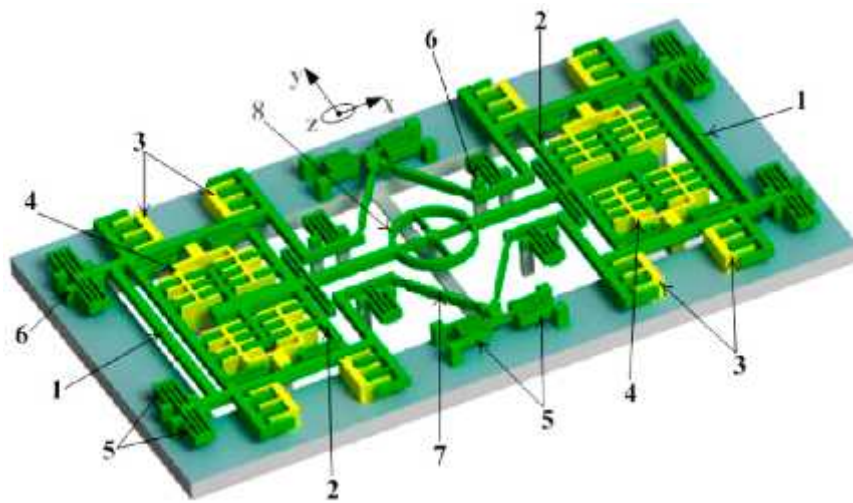
. [43].

.1.11.

9,78 9,76

111,2,

11,56 / / .



1.11.

z [43]:

1—

, 2—

, 3—

, 4—



,5—

,6—

,7—

8—

Guan . [44]

,

.

.

,

.

,

4006

4464

,

5958

,

50%

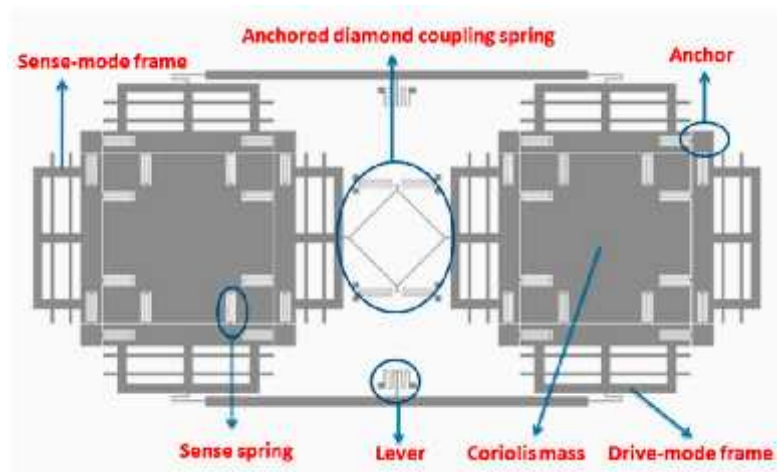
,

[45]

,

,

.1.12.



1.12.

[45].

310 k

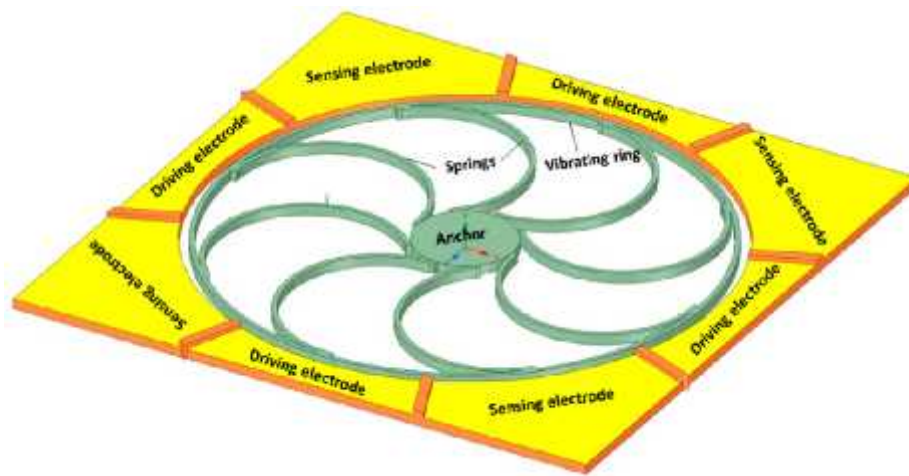
640 k

[46].

1.2.3.

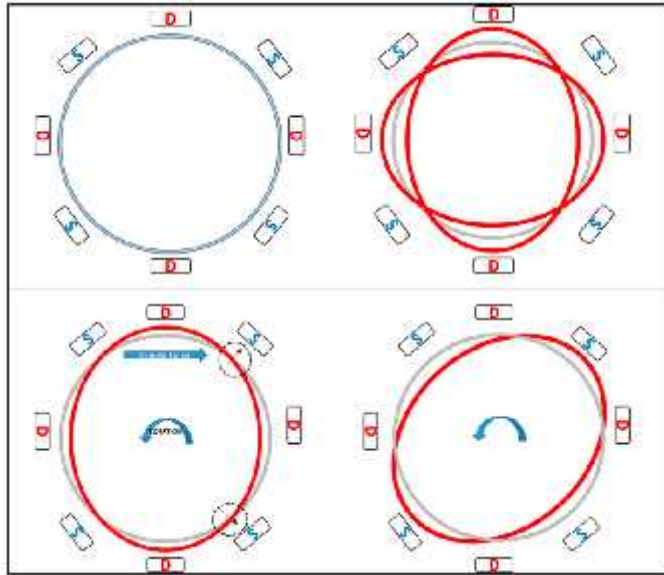
[47].

.1.13.



1.13.

.1.14..



1.14.

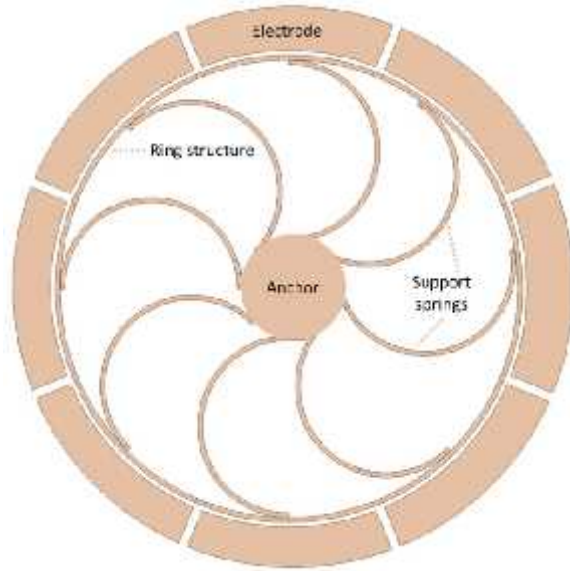
### General Motors

[48].

.1.15.

45

45



1.15.

General Motors.

1998

[49].

30 40 ,

0,9 .

[50]

30

0,9 . ARW

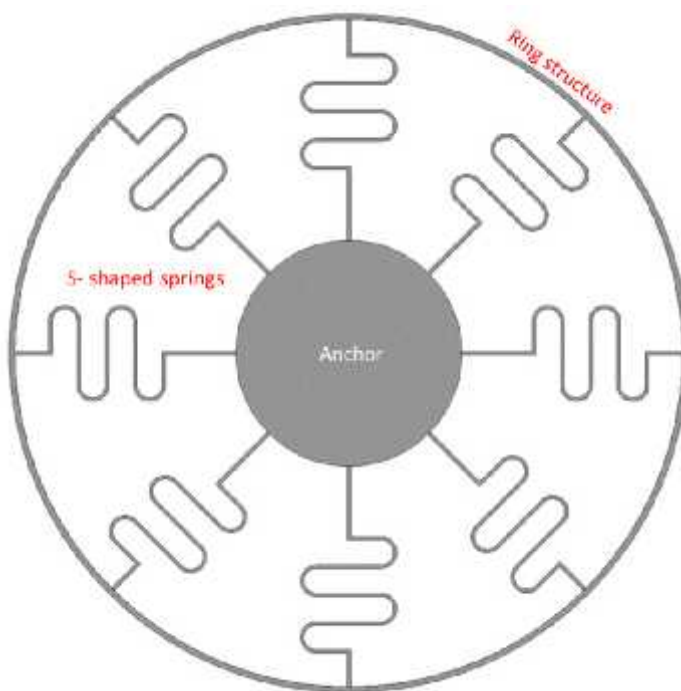
$$0,05 \frac{\text{град}}{\sqrt{n}}$$

[51]

80 .  
 ,  
 200  
 / / ±250 /  
 . 1200,  
 0,15 2 .  
 (111)  
 . [52].  
 1,35 , 150  
 . DRIE 480  
 (111). 150 .  
 ,  
 12 000, 0,02%,  
 132 / / .  
 . [53]. S-  
 ,  
 .1.16.  
 ,  
 .  
 9,844 9,865  
 186 163

0,017 / , ARW

0,14  $\frac{\text{град}}{\sqrt{h}}$ .



1.16.

S-

[54].

6,04 ,

Syed . [55]

0,0036 / / .

C-

, ' ,

C-

. ,

. ; ,

. ,

,

.

. [56].

.  
U-

, ' ,

, ,

.

.

U-

.1.17.

9,609

9,615

;

9,124

9,146

,

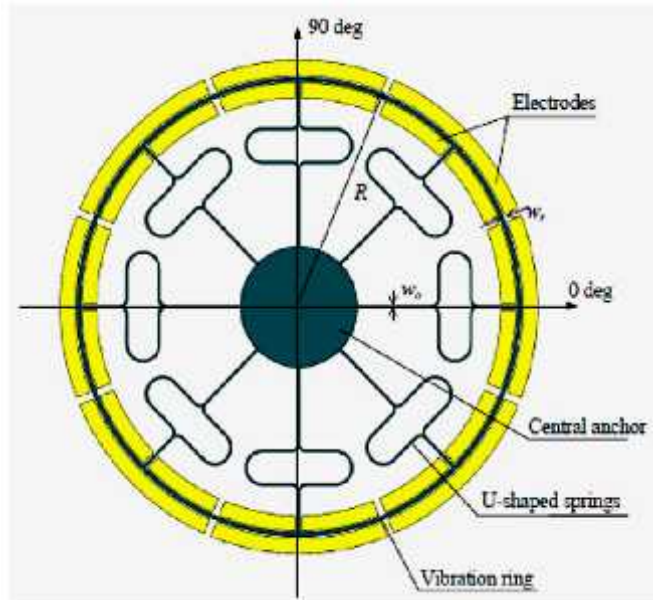
8,86

/

,

ARW

0,78  $\frac{\text{град}}{\sqrt{h}}$ .



1.17.

U- [56]

[57].

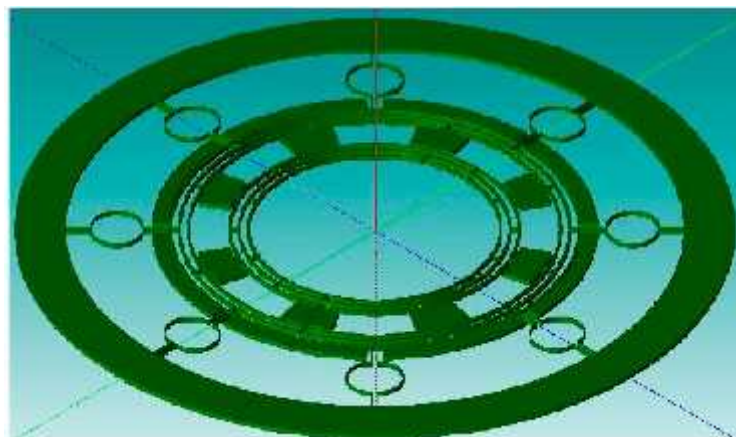
C-

1.18.

40,40

36,67

4,0





1.18.

[57].

Liang . [58]

[59]

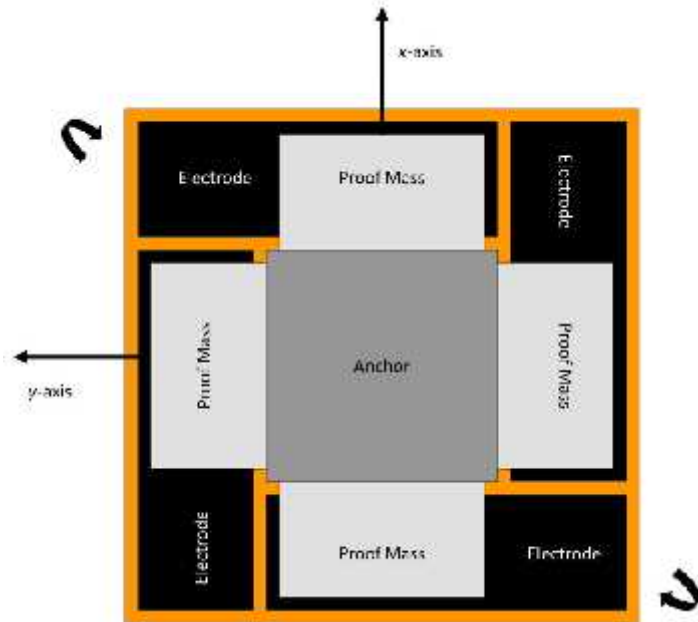
**1.2.4.**

Fujita

. [60].

.19,

0,1 / / .



1.19.

Fujita

1997

IEEE Transducers 97 Conference [ 61 ]

1,6

2

0,3

z,

x

y.

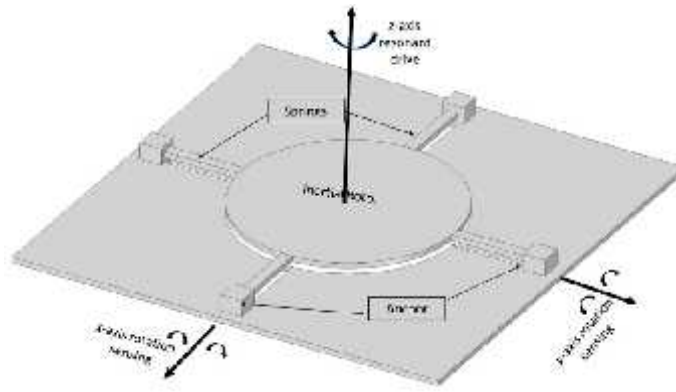
y

x.

.1.20. ARW

, ARW

$$2 \frac{\text{град}}{\sqrt{\text{год}}} \quad 10 \frac{\text{град}}{\sqrt{\text{год}}}$$



.1.20.

NASA

,  
[62].

7

,  
70 / , ARW

24 / / ,  
6,3  $\frac{\text{град}}{\sqrt{\text{ГОД}}}$

1998  
.[63].

,

2 .

/ 100 [64,65].

X-Y.

-40 °C 100 °C [66].

Senkal . [28]

.1.21.

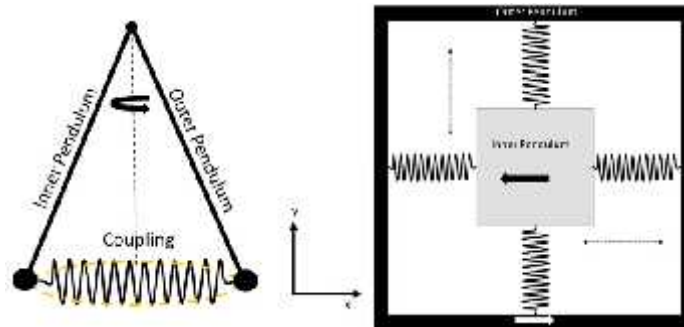
X-Y.

2,7

100

. [67]

24



1.21.

. 1.1

	[31] ,	1988		350 × 500
	[33] ,	1996	/ 360	
	[35] ,	1999	/ 65	
	[36] ,	2005		
	[38] ,	2019		
	[34] ,		/ 100	
	[42] ,		81 000 64 000	
	[41] ,			
	[44] ,		/ / 11,56	50%.

	[43]		11,56 / /	z
	[68]		0,59 / 0,04 $\frac{\text{град}}{\sqrt{\text{год}}}$	100 ±200 /
	[69]		9,27 / 0,923 $\frac{\text{град}}{\sqrt{\text{год}}}$	3D- 52 000 49 300
	Si-Ware Systems, [70]		5,5 / 0,2 $\frac{\text{град}}{\sqrt{\text{год}}}$	
	General Motors Corporation, [48]	1995		
	[49]	1998	0,05 $\frac{\text{град}}{\sqrt{\text{год}}}$	30 40
	[52]	2002	132 / 12 000 /	(111). 1,35 150
	[71]	2015	80 000 250	600
	[72]	2015	100 k 20 ppm	1760
	[53]	2017	61,2 /	S-
	[55]	2019		
	[56]	2019	8,86 /	U-

	[58]	2020		
	[73]	2020	64,89 64,91	
	[74]	2020		
	[19]	2021		(100)
	[60]	1997	0,1 / /	
	UC Berkeley, [61]	1997	$2 \frac{\text{град}}{\sqrt{\text{год}}}$	$0,3^2$ 1,6
	[63]	1998		
	[75]	2005	,74 fF/ / 19,4 fF/ /	
	[64]	2011	$\pm 450$ / 100	2
		2012	1,1	

	[66]		-40 °C 100 °C.	
	[76]	2013	1 ppm  10 °C	
	[28]	2015		
	[77]	2020	100 k  2,7	25,44
	[78]	2020	1,75 / / ,  41,4 /	
	[23]	2021		FEA.



2.1.

,

2.1.1.

.

(VCG)

.

[79].

VCG. . . .

2

,

VCG [80, 81].

.

,

/

[82]. . . .

[83].

, .

[9], -

[84]. Ethem Erkan Aktakka

[85].

[86]. . .

[87]. Yanqi Liu Jihyun Cho

[88, 89].

[90].

VCG,

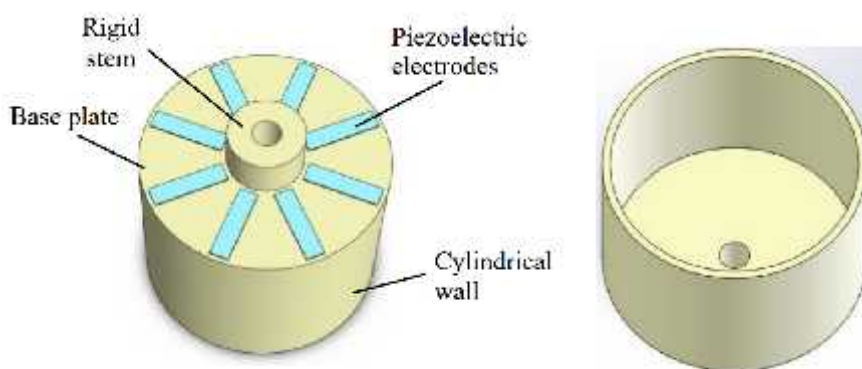
VCG

**2.1.2.**

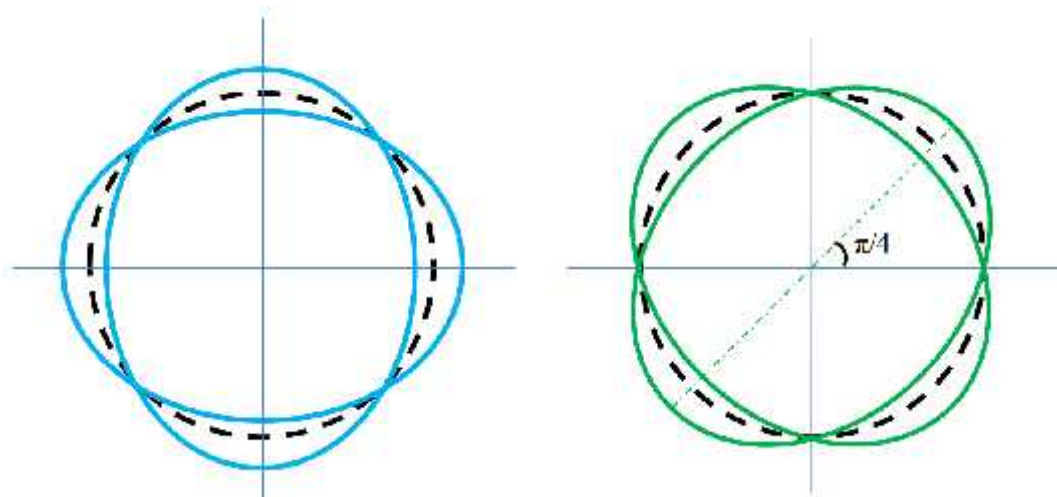
.2.1[91].

.2.2(a).

[92],



2.1.



2.2.

2.1.3.

[93].

[87]:

$$\sigma = E(e + a_3 e^3) \# (2.1)$$

$a^3$  —

$e; E$  —

$$F(x) = k + \epsilon x^3 \# (2.2)$$

$x$  —

,  $kx$  —

,  $x^3$  —

(2.3)

$$k + \epsilon x^3 = -m\ddot{x} \# (2.3)$$

$$\ddot{x} + \omega_n^2 x + \mu x^3 = 0 \# (2.4)$$

$$\begin{aligned} x(0) &= A \\ \dot{x}(0) &= 0 \end{aligned} \# (2.5)$$

$$\mu = \frac{\varepsilon}{m}$$

$\mu=0$ ,

[94]:

$$x = A \cos \omega t + \mu \frac{A^3}{32\omega^2} (\cos 3\omega t - \cos \omega t) \quad \#(2.6)$$

$$\omega = \omega_n \sqrt{1 + \frac{3\mu A^2}{4\omega_n^2}} \approx \omega_n \left(1 + \frac{3\mu A^2}{8\omega_n^2}\right) \quad \#(2.7)$$

(2.7)

A

$\mu$ .

$\mu > 0$

( )

$\mu < 0$  –

( ) [93].

#### 2.1.4.

#### VCG

0,

VCG

VCG,

[94].

$$\begin{aligned} \ddot{x} - 4k \dot{y} + \left(\frac{2}{l} + \Delta \frac{1}{l} \cos 4\theta_i\right) \dot{x} + \Delta \frac{1}{l} \sin 4\theta_i \dot{y} + (\omega^2 + \omega \Delta \cos 4\theta_\omega) x - \omega \Delta \sin 4\theta_\omega y &= F_x \\ \ddot{y} - 4k \dot{x} + \left(\frac{2}{l} - \Delta \frac{1}{l} \cos 4\theta_i\right) \dot{y} + \Delta \frac{1}{l} \sin 4\theta_i \dot{x} + (\omega^2 - \omega \Delta \cos 4\theta_\omega) y - \omega \Delta \sin 4\theta_\omega x &= F_y \end{aligned} \quad \#(2.8)$$

$$\omega^2 = \frac{\omega_1^2 + \omega_2^2}{2}, \quad \frac{1}{\tau} = \frac{1}{2} \left( \frac{1}{\tau_1} + \frac{1}{\tau_2} \right), \quad \omega \Delta \omega = \frac{\omega_1^2 - \omega_2^2}{2}, \quad \Delta \frac{1}{\tau} = \frac{1}{\tau_1} - \frac{1}{\tau_2}$$

(2.8) x, y — X Y, F\_x F\_y

$$\begin{aligned} \ddot{x} + c_1 \dot{x} + c_2 \dot{y} + k_1 x + k_2 y &= F_x \\ \ddot{y} + c_2 \dot{y} + c_1 \dot{x} + k_2 y + k_1 x &= F_y \end{aligned} \quad (2.9)$$

$$\begin{aligned} c_1 &= \frac{2}{\tau} + \frac{\Delta 1}{\tau} \cos 4\theta_\tau = \left( \frac{1}{\tau_1} + \frac{1}{\tau_2} \right) + \left( \frac{1}{\tau_1} - \frac{1}{\tau_2} \right) \cos 4\theta_\tau \\ c_2 &= c_1 = \frac{\Delta 1}{\tau} \sin 4\theta_\tau = \left( \frac{1}{\tau_1} - \frac{1}{\tau_2} \right) \sin 4\theta_\tau \\ c_2 &= \frac{2}{\tau} - \frac{\Delta 1}{\tau} \cos 4\theta_\tau = \left( \frac{1}{\tau_1} + \frac{1}{\tau_2} \right) - \left( \frac{1}{\tau_1} - \frac{1}{\tau_2} \right) \cos 4\theta_\tau \\ k_1 &= \omega^2 + \omega \Delta \omega \cos 4\theta_\omega = \frac{\omega_1^2 + \omega_2^2}{2} + \frac{\omega_1^2 - \omega_2^2}{2} \cos 4\theta_\omega \\ k_2 &= -\omega \Delta \omega \sin 4\theta_\omega = -\frac{\omega_1^2 - \omega_2^2}{2} \sin 4\theta_\omega \\ k_1 &= \omega^2 - \omega \Delta \omega \cos 4\theta_\omega = \frac{\omega_1^2 + \omega_2^2}{2} - \frac{\omega_1^2 - \omega_2^2}{2} \cos 4\theta_\omega \end{aligned}$$

$$F_y = 0,$$

$$(2.9) :$$

$$\begin{aligned} (s^2 + c_1 s + k_1)X(s) + (c_2 s + k_2)Y(s) &= F_x(s) \\ (s^2 + c_2 s + k_2)Y(s) + (c_1 s + k_1)X(s) &= 0 \end{aligned} \quad (2.10)$$

$$(2.10) :$$

$$X(s) = \frac{s^2 + c_2 s + k_2}{(s^2 + c_2 s + k_2)(s^2 + c_1 s + k_1) - (c_2 s + k_2)(c_1 s + k_1)} F_x(s) \quad \#(2.11)$$

$$Y(s) = -\frac{c_1 s + k_1}{(s^2 + c_2 s + k_2)(s^2 + c_1 s + k_1) - (c_2 s + k_2)(c_1 s + k_1)} F_x(s)$$

$$Z_\theta(s) = X(s) \cos 2\theta + Y(s) \sin 2\theta \quad \#(2.12)$$

CVG

PZT

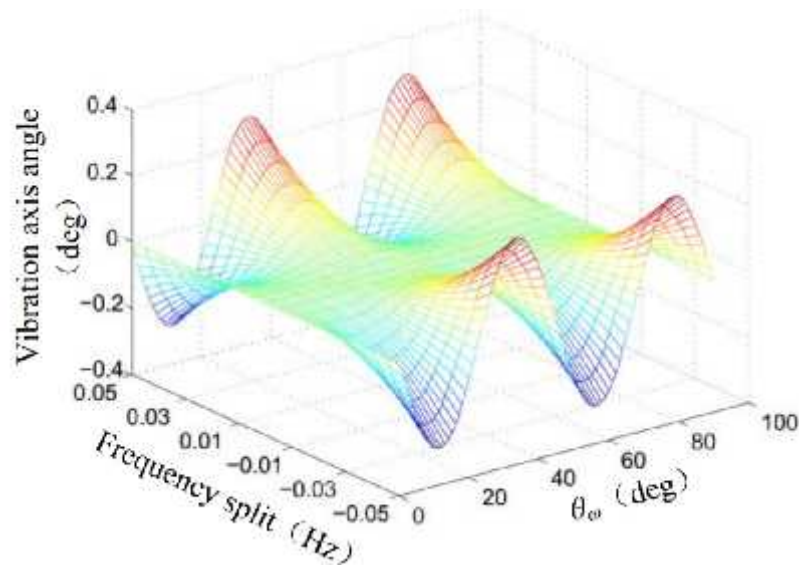
VCG.

3,

$$f_1=5000, Q_1=Q_2=10000$$

(2.12),

.2.3.



2.3.

.2.3,

2.1.5.

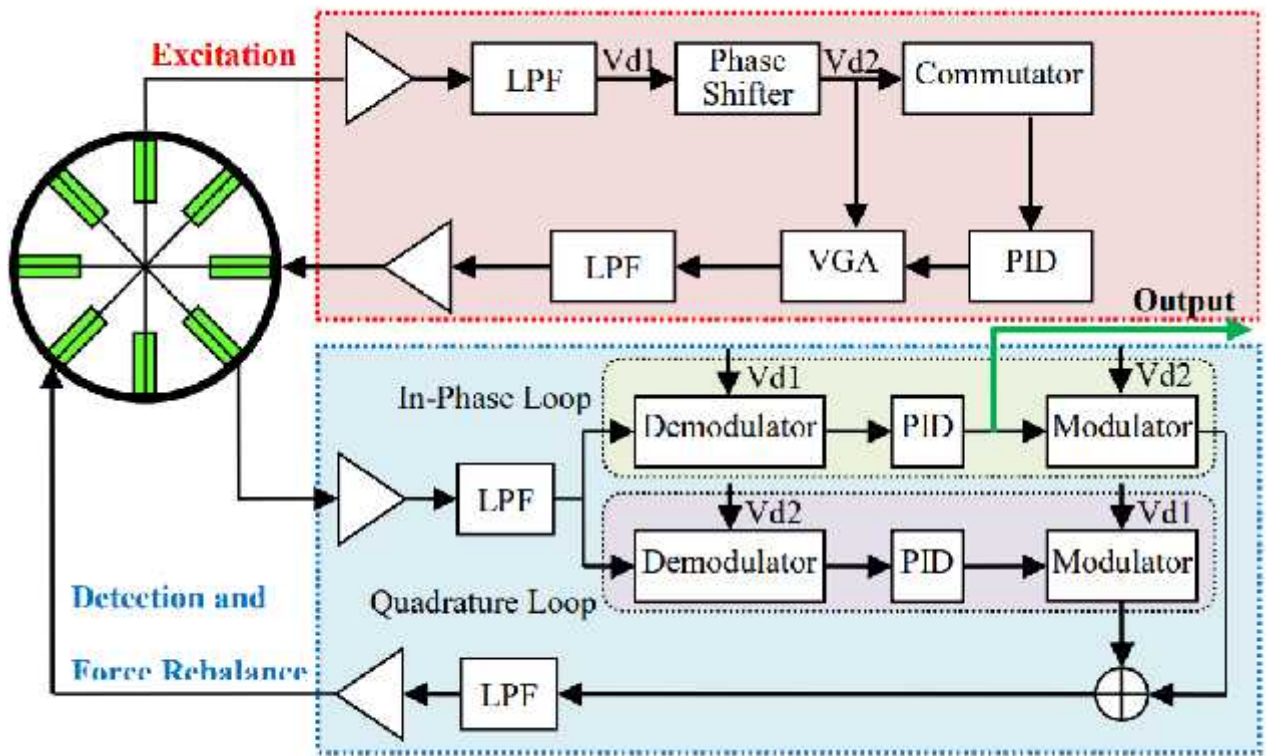
[95,96].

,  $\omega_1 \approx \omega_2$ .

VCG,

. 2.4.





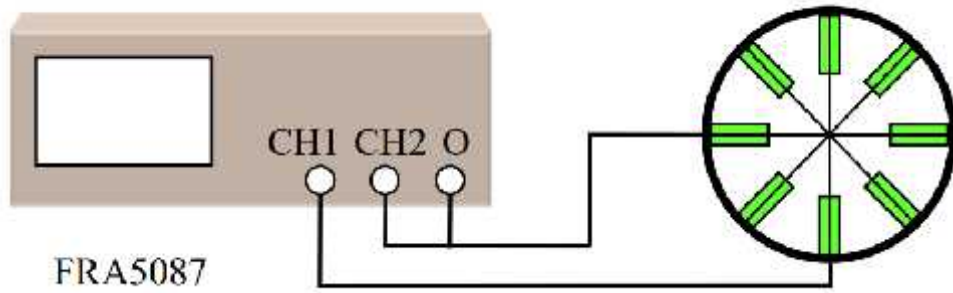
2.4. - VCG

2.1.6.

NF FRA5087.

.2.5, FRA5087

FRA. CH1 CH2  
 90°



2.5.

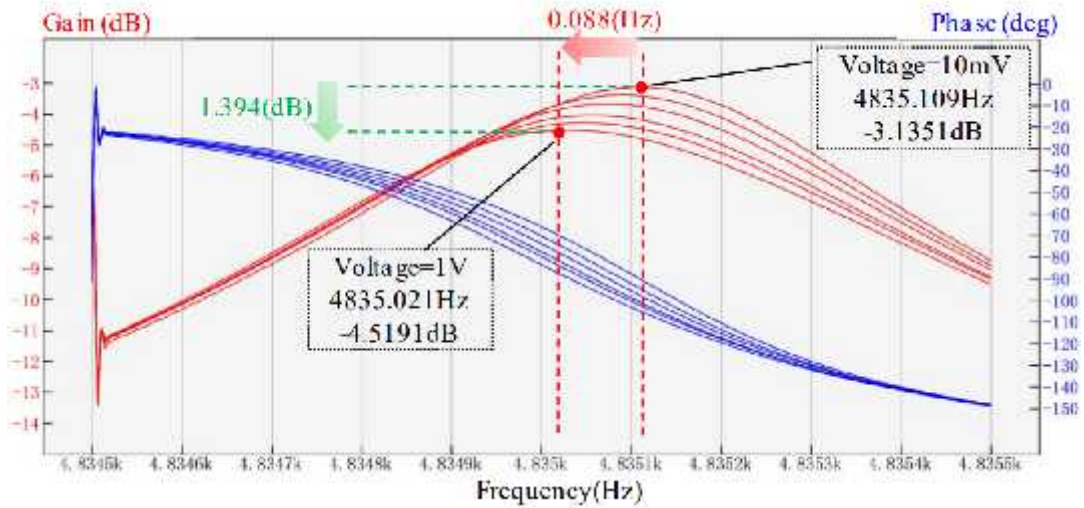
[99]

FRA5087 10

1 ,

.2.6,

«Gain» CH1/CH2.



2.6.

.2.6

10

1 ,

4835,109

4835,021 ,

-3,1351

-4,5191 .

0,088

VCG

VCG.

### 2.1.7.

2.1.4,

0

.2.7,

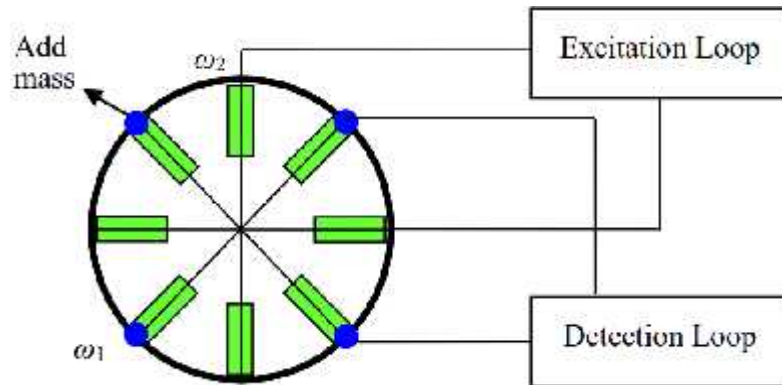
1

2

$$\omega_1 > \omega_2$$

.2.7,

1.



2.7.

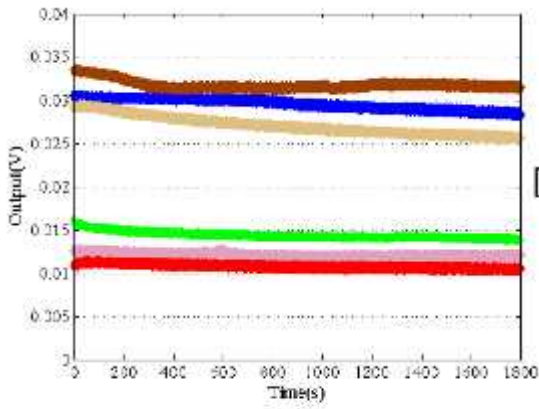
[99]

$$(\Delta\omega = \omega_1 - \omega_2)$$

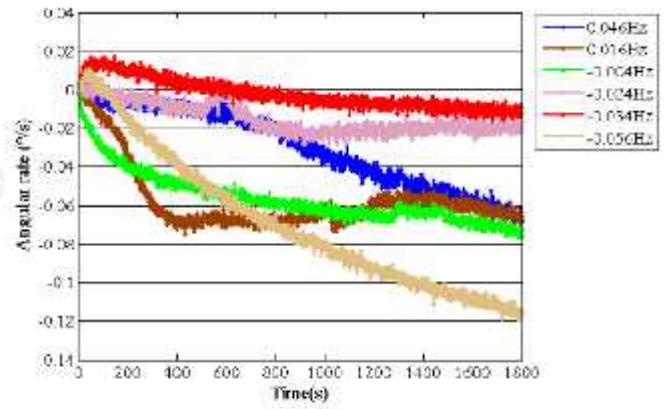
-0,056

0,046

.2.8(a)

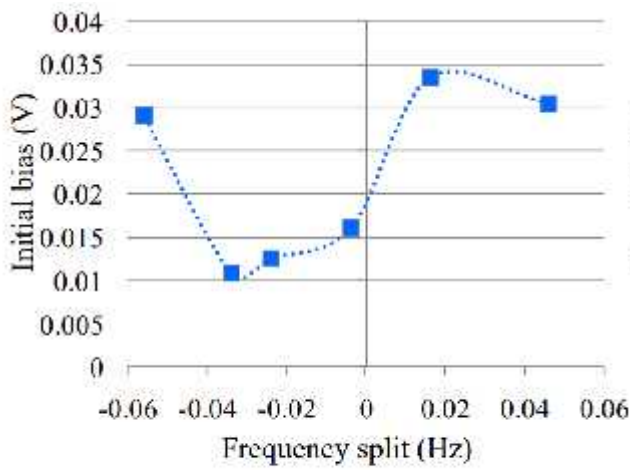


(a)

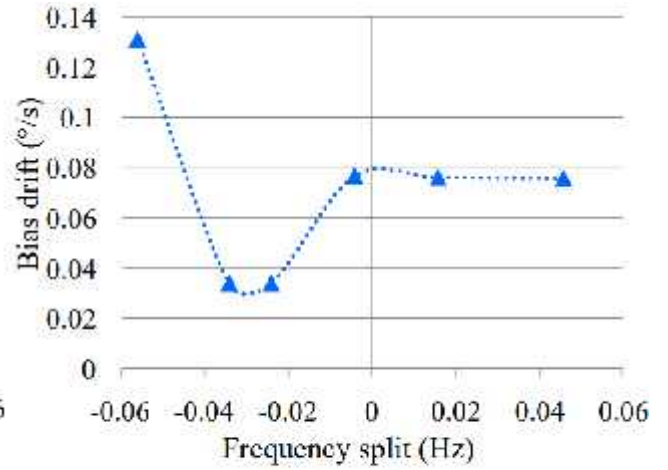


(b)

2.8.



(a) Initial bias



(b) Bias drift

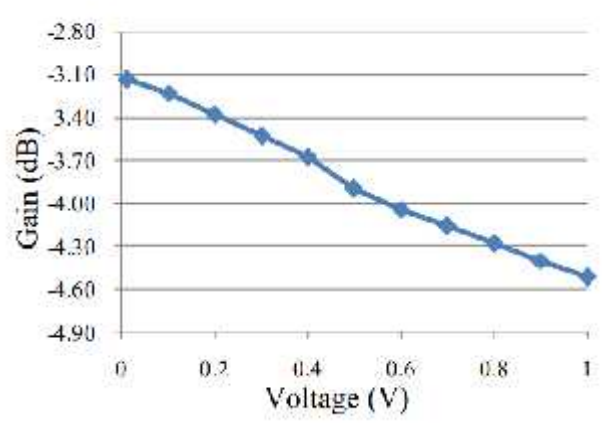
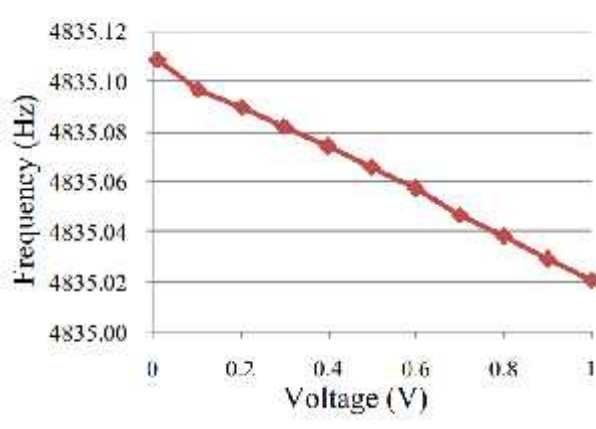
2.9.

.2.8(a)

.2.9(a),

(-0,004 ),  
-0,034 .  
.2.8(b) .2.9(b)  
(0,13% / ),  
( 0,025% / ),  
(-0,004 )

500  
50  
50  
0,3  
.2.10(a),  
-0,34 -0,24 .

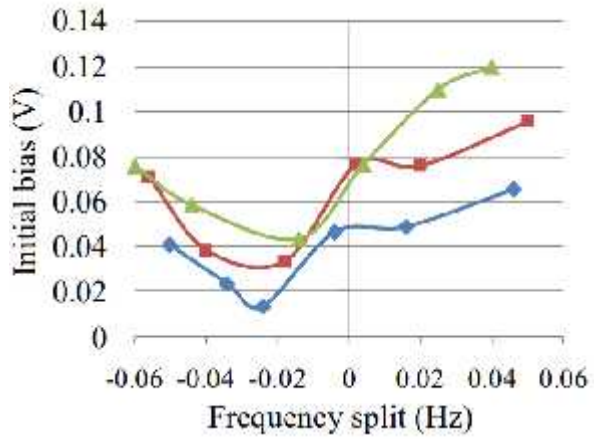


2.10.

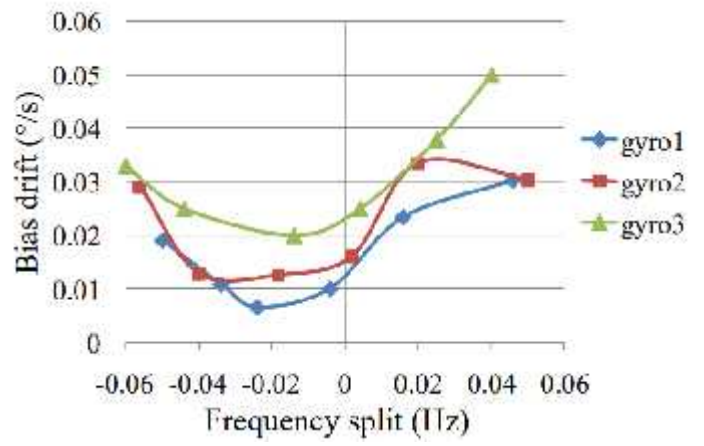
[99]

PZT

.2.11.



2.11.



.2.11,

2.2.

2.2.1.

$$V_s = \frac{1}{K} \sqrt{\frac{1}{n-1} \sum_{i=1}^n (F_i - \bar{F})^2}$$

K — , F — ,  
 F<sub>i</sub> — t<sub>i</sub>. K=1,  
 ,  
 ,  
 - — - ,  
 -  
 ,  
 ,  
 ,  
 KALMAN -

### 2.2.2. ARMA

: {x<sub>t</sub>},  
 , n  
 {x<sub>t-1</sub>}, {x<sub>t-2</sub>}, ..., {x<sub>t-n</sub>} m  
 {a<sub>t-1</sub>}, {a<sub>t-2</sub>}, ..., {a<sub>t-m</sub>} {x<sub>t</sub>},  
 ARMA  
 :  

$$x_t = \phi_1 x_{t-1} + \phi_2 x_{t-2} + \dots + \phi_n x_{t-n} - \theta_1 a_{t-1} - \theta_2 a_{t-2} - \dots - \theta_m a_{t-m} + a_t$$
 i (i = 1,2,3,...,n) - , j (j = 1,2,3,...,m) -  
 , {a<sub>t</sub>} -  
 x<sub>i</sub>, ARMA(n, m) .

ARMA (n, m)

:

AIC.

j, k,

2

AIC:

$$A(k, j) = \ln(\delta^2(k, j)) + \frac{2(k + j)}{N} \quad \#(33)$$

(p', q') AIC (k, j)

AIC (p, q),

ARMA (p, q).

ARMA

(p, q)

$x_1, x_2, \dots, x_N$ :

AR,

$$P = \lfloor \sqrt{N} \rfloor, \lfloor \sqrt{N} \rfloor -$$

N.

P

AR

$(a'_1, a'_2, \dots, a'_p)$

AIC.

:  $\varepsilon = x_t -$

$$\sum_{j=1}^p a'_j x_{t-j}, \quad (t = p + 1, p + 2, \dots, N).$$

ARMA (p, q):

$$x_t = \sum_{j=1}^p a_j x_{t-j} + \varepsilon + \sum_{j=1}^q b_j \varepsilon_{t-j}$$

$$t = L + 1, L + 2, \dots, N, \quad L = \max(p', p, q), \quad a \quad b -$$

ARMA.

:

$$Y = \begin{bmatrix} x_{L+1} \\ x_{L+1} \\ \dots \\ x_{L+1} \end{bmatrix} \quad \#(2.14)$$

$$Y = \begin{bmatrix} x_L & \dots & x_{L-p+1} \\ \vdots & \ddots & \vdots \\ x_{N-1} & \dots & x_{N-p} \end{bmatrix} \quad \#(2.15)$$



$$\varepsilon = \begin{bmatrix} \varepsilon'_L & \cdots & \varepsilon'_{L-q+1} \\ \vdots & \ddots & \vdots \\ \varepsilon'_{N-1} & \cdots & \varepsilon'_{N-q} \end{bmatrix} \#(2.16)$$

$$\beta = [a, b]^T$$

:

$$\beta = \begin{bmatrix} X^T X, X^T \varepsilon \\ \varepsilon^T X, \varepsilon^T \varepsilon \end{bmatrix}^{-1} \begin{bmatrix} X^T Y \\ \varepsilon^T Y \end{bmatrix} \#(2.17)$$

:

$$Q(a, b) = \sum_{t=L+1}^N \left( x_t - \sum_{j=1}^p a_j x_{t-j} - \sum_{j=1}^q b_j \varepsilon_{t-j} \right)^2 \#(2.18)$$

$$\sigma'^2 = \frac{Q(a, b)}{N-L} \#(2.19)$$

:

)

:

$$X_k = AX_k + BV_k \#(2.20)$$

)

:

$$Y_k = CX_k + W_k \#(2.21)$$

$$V_k \quad W_k, \quad E(W_k) =$$

$$0, \quad E(V_k) = 0, \quad E(W_k W_j^T) = Q_k \delta_{kj}, \quad E(V_k V_j^T) = R_k \delta_{kj}, \quad E(W_k V_j^T) = 0.$$

$$X_k = [\hat{x}_k, \hat{x}_{k-1}]^T, \quad V_k = [a_k, 0]^T.$$

$$W_k, \quad X_k = \hat{x}_k + W_k.$$

$$Y_k = x_k, \quad : \quad Y_k = CX_k + W_k;$$

$$V_k \quad W_k$$

$$V_k \quad W_k$$

$$\cdot \quad ,$$

:

$$\begin{cases} \bar{X}_{k,k-1} = A\bar{X}_{k-1,k-1} \\ \bar{X}_{k,k} = \bar{X}_{k,k-1} + K_k[Y_k - C_k\bar{X}_{k,k-1}] \\ K_k = P_{k,k-1}C^T[CP_{k,k-1}C^T + R_k]^{-1} \\ P_{k,k-1} = AP_{k,k-1}A^T + BQ_{k-1}B^T \\ P_{k,k} = [I - K_kC]P_{k,k-1} \\ \bar{Y}_k = C\bar{X}_{k,k} \end{cases} \quad \#(2.22)$$

(2.22)  $\bar{X}_{k,k-1}$  — ,  $\bar{X}_{k,k}$  —

$k, K_k$  —

$k, R$  —

,  $Q$  —

,  $P_{k,k}$  —

,  $\bar{Y}_k$  —

$k$ .

### 2.2.3.

(MALLAT)

a

b CWT

DWT ( $a = a_0^m, b = nb_0a_0^m, m, n \in \mathbb{Z}$ ).

$$\psi_{m,n}(t) = |a|^{-\frac{m}{2}} \psi(a_0^{-m}t - nb_0) \quad m, n \in \mathbb{Z}$$

$$\psi_{a,b}(t) = |a|^{-\frac{1}{2}} \psi\left(\frac{t-b}{a}\right).$$

$$(W_\psi f)(a,b) = \int_{-\infty}^{\infty} f(t) \overline{\psi(a_0^{-m}t - nb_0)} dt \quad \#(2.23)$$

,  $a_0 = 2, b_0 = 1,$

$a = 1, 2^1, 2^2, \dots, 2^J,$

:

$$\psi_{m,n}(t) = 2^{-\frac{m}{2}} \psi(2^{-m}t - n) \quad m, n \in \mathbb{Z} \quad \#(2.24)$$

,

,

-

:

$$\psi_{m,n} \psi_{j,k} = \int_{-\infty}^{\infty} \psi_{m,n}(t) \overline{\psi_{j,k}(t)} dt = \delta_{m,j} \delta_{n,k} \quad (2.25)$$

$$x^1 = x_k^{(0)} \cdot h(k) = \sum_n h(k-n) x_n^{(0)}, \quad x_k^{(0)} = \sum_n h(k-n) x_n^1$$

$$d_k^1 = \sum_n h_0(n-2k) x_n^{(0)}, \quad d_k^1 = \sum_n h_1(n-2k) x_n^{(0)}$$

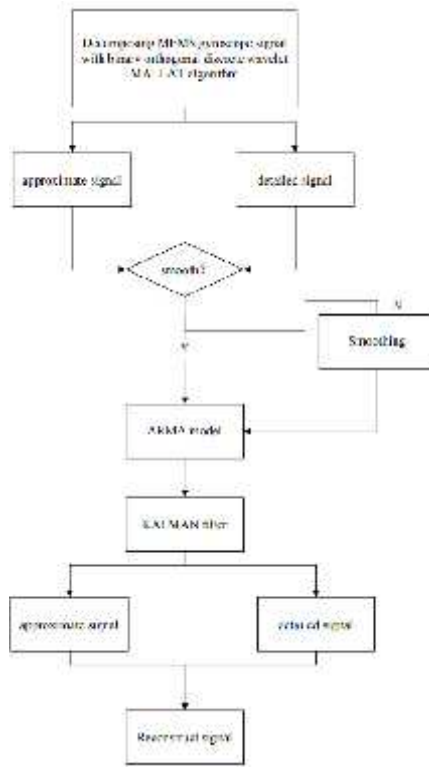
MALLAT.

#### 2.2.4.

MALLAT,

ARMA

KALMAN,



2.12.

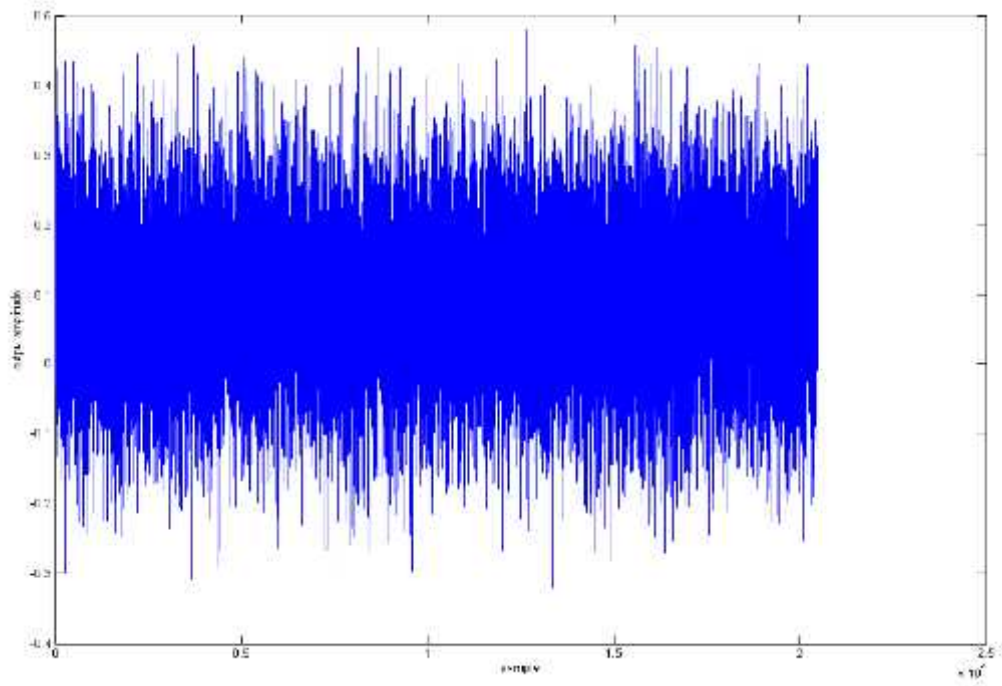
2.2.5.

[100]

GJB\_2426A-2004,

X

.2.13.



2.13.

1

GJB\_2426A-2004,

7,5901 (°)/ .

- [100]

-

,

:

1.

,

;

2.

:

,

-

;

3.

,

,

-

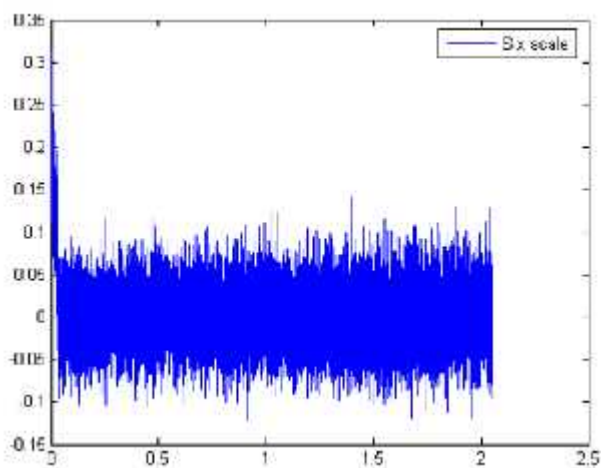
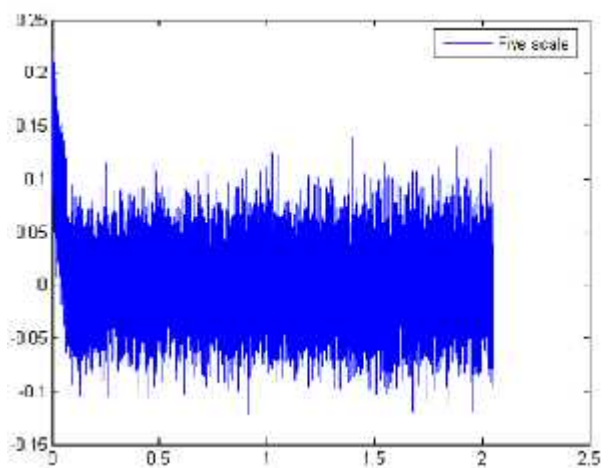
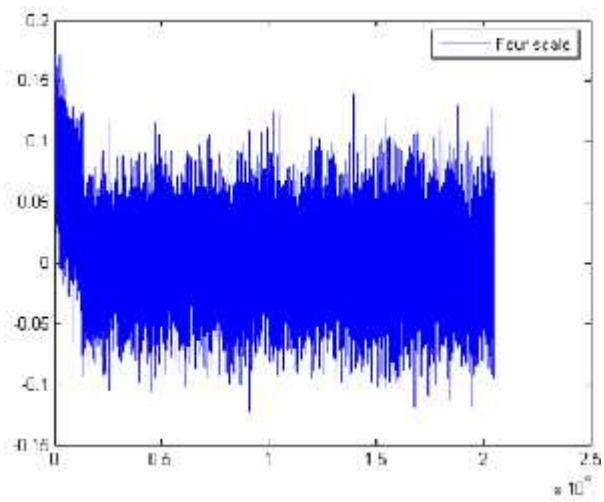
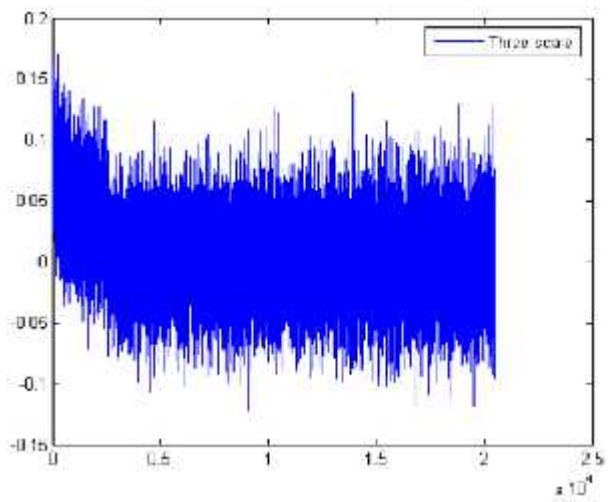
.

-

,

:

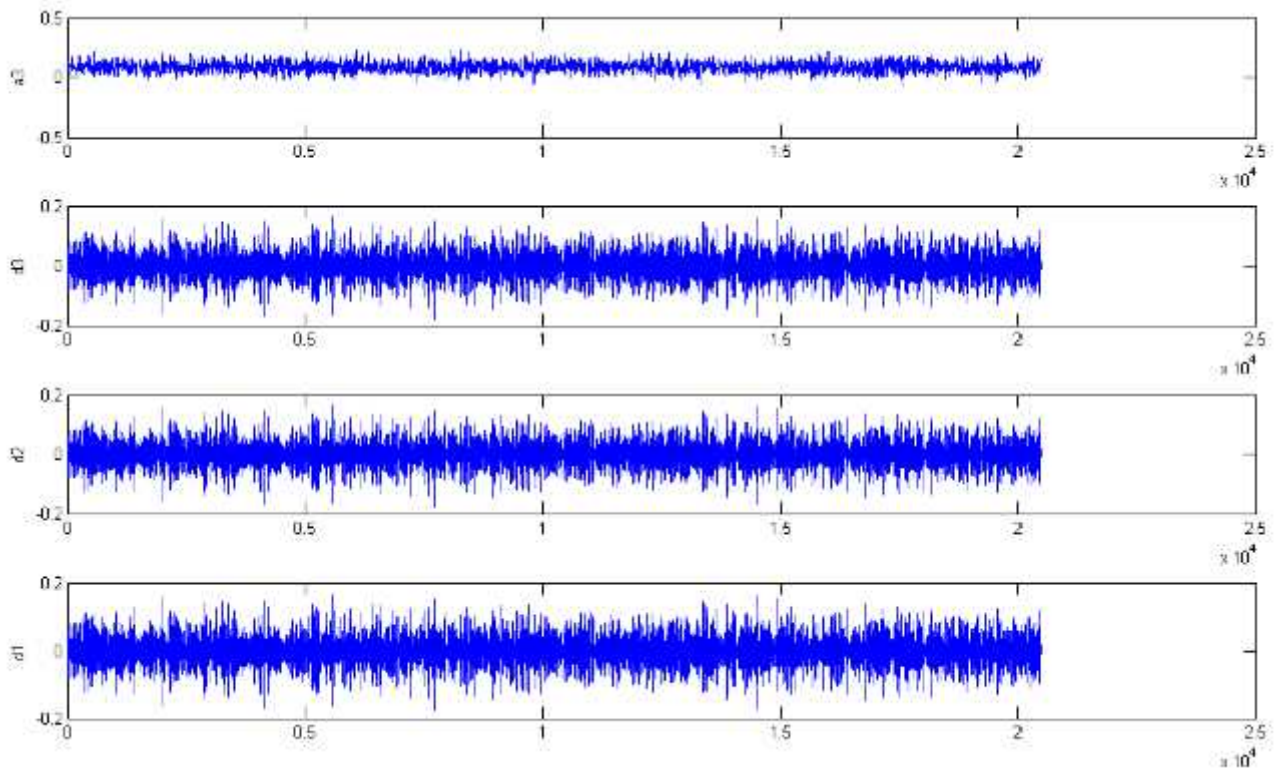
) : dbN (N=1,2,...,10),  
 ,  
 ,  
 . Db5.  
 ) - : -  
 bior Nr.Nd.  
 ,  
 ,  
 ,  
 FIR.  
 ,  
 .  
 Biorl.5.  
 ) : , dbN,  
 Coif3 coifN(N=1,2,3,4,5).  
 :  
 ,  
 .  
 ,  
 SymN(N=2,3,...,8).  
 Sym5.  
 [100]  
 ,  
 ,  
 .  
 .  
 .2.14 - db5 .



2.14.

Db5  
- MALLAT,

.2.15.

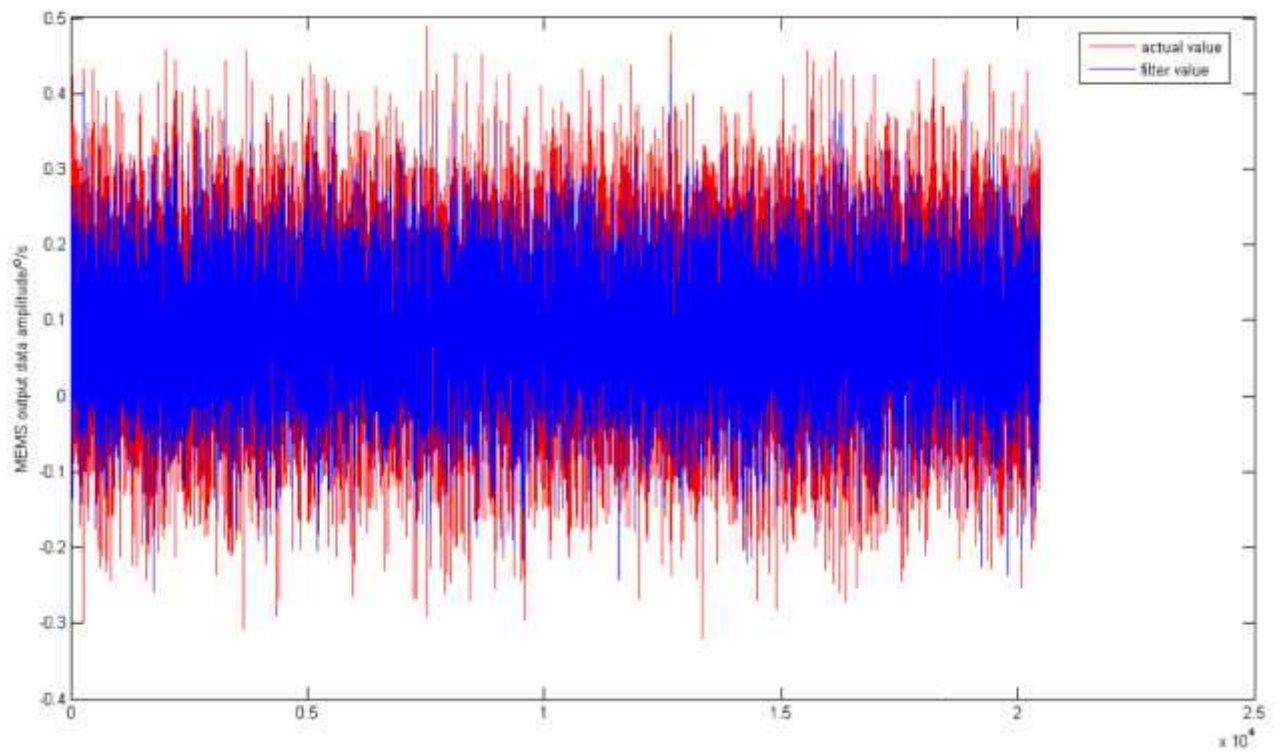


2.15.

ARMA

.2.14

.2.16.



2.16.



3,7957 (°)/ ,

### 2.3.

#### 2.3.1.

PZT,

$$\sigma = E T \#(2.26)$$

$E$  — ,  $a$  —

,  $T$  —

{  $G$  } —

$$\{G\} = \{G_0\}(1 + a T) \#(2.27)$$

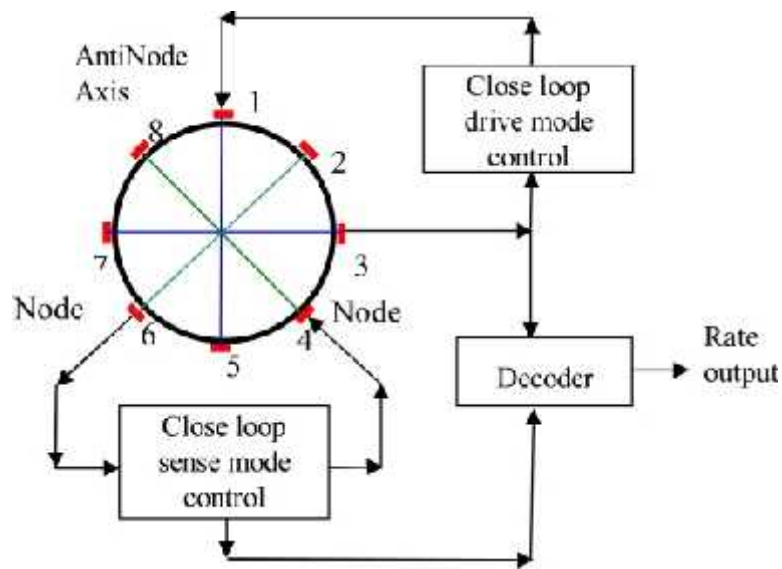
{  $G_0$  } —

$$\sigma = E \left( \frac{\{G\}}{\{I_0\}} - 1 \right) \#(2.28)$$

$V_{dd}$

,  $V_{ds}$

:



2.17.

$$V_a = V_1 \sin(\omega t), \quad V_d = V_2 \sin\left(\omega t - \frac{\pi}{2}\right) \#(2.29)$$

$V_1$   $V_2$ —

$V_{ss}$ :

$$V_s = V_3(\Omega) \sin\left(\omega t - \frac{\pi}{2}\right) \#(2.30)$$

2.17.,

1-5

3-7,

2-6

$V_3(\ ) -$  ,  
 $V_{ds} V_{ss}$  ,  
 $V_{ds}$  .  
 2-6, 4-8  
 1-5, 3-7  
 2-6 ,  $V_{ss0}$   
 $= 0$ .  
 node axes antinode axes 1 (NodeAxis1) 1  
 (AntiNode Axis1), , 1, .2.18.

1-5, 3-7 .  
 3-7 ,  
 [101]

:

$$V'_a = \frac{V_2}{\cos 2\theta_1} \sin\left(\omega - \frac{\pi}{2}\right) = V'_2 \sin\left(\omega - \frac{\pi}{2}\right) \#(2.31)$$

,  
 2-6, 4-8, ,  $V_{ss0}$   
 :

$$V_{s,0} = V'_2 \cos 2\left(\frac{\pi}{4} - \theta_1\right) \sin\left(\omega - \frac{\pi}{2}\right) = V_2 \tan 2\theta_1 \sin\left(\omega - \frac{\pi}{2}\right) \#(2.32)$$

(46) (48)

, , ,  
 , , .  
 (48) ,

$V_{ss0}$

, 1.

. , ,

$$[102], \quad (V_2/100)/(\text{°/}). \quad (48)$$

,  
 $1^\circ$ ,  
 $3,5\%$  . ,  
 ;

### 2.3.2.

[103].

ANSYS.

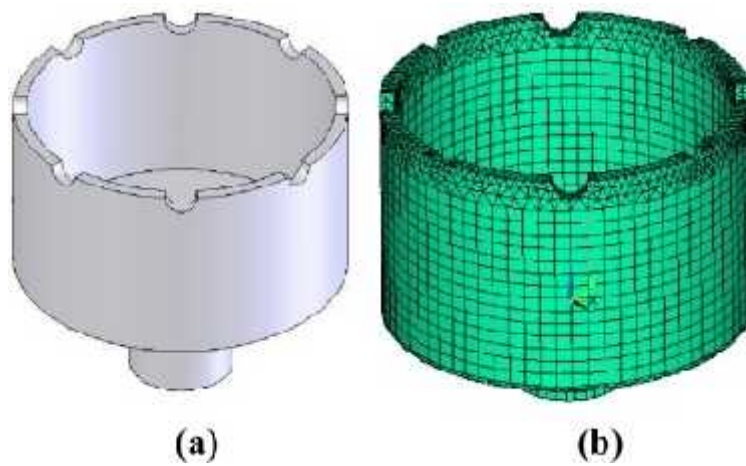
[103].

.2.18,

25 ,

1 ,

15



2.18. (a)

. (b)

. 2.1.

-40 °C 60 °C.

2.1

	( / <sup>3</sup> )	( )	(1/°C)	(1/°C)	
	8250	220	$10^{-5}$	$10^{-5}$	0,3

, ANSYS

solid 95,

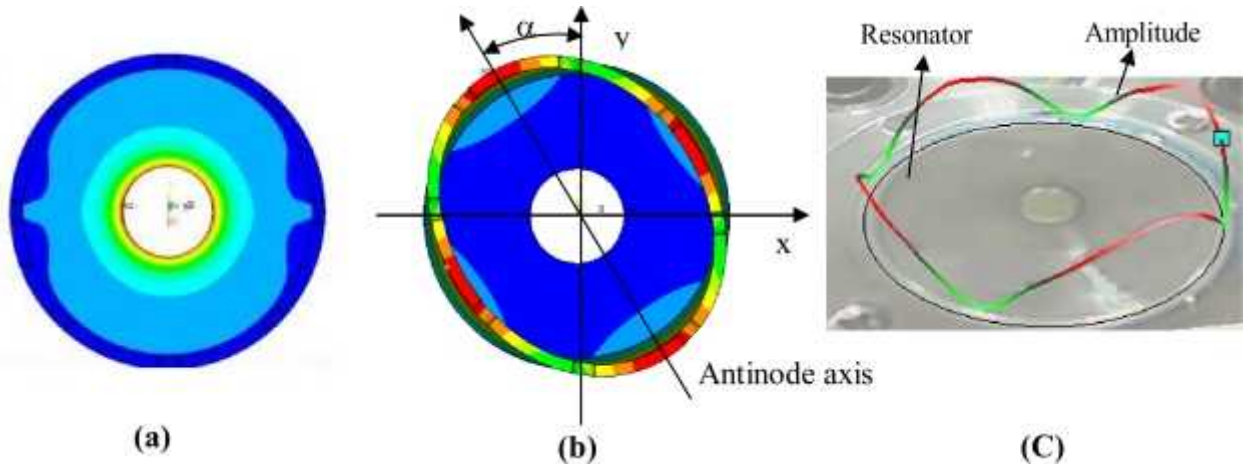
20

7396

.2.18(b).

1

.2.19( ).



(a)

(b)

(c)

2.19.( )

. (b)

. (C)

.2.19(b) [103].

0 °C

5253,15

.2.19(c)..

Polytec400,  
5151,33 ,

2.3.3.

1 0 °C.  
 4,  
 -40 °C, -20 °C, 0 °C, 20 °C, 40 °C 60 °C.

.2.2.

2.2

	-40°	-20°	0°	20°	40°	60°	
	22,24°	22,84°	23,40°	23,47°	24,93°	25,47°	3,23°

.2.2 , -40 °C 60 °C,  
 3,23°,

11,3°/

2.3.4.

.2.18,

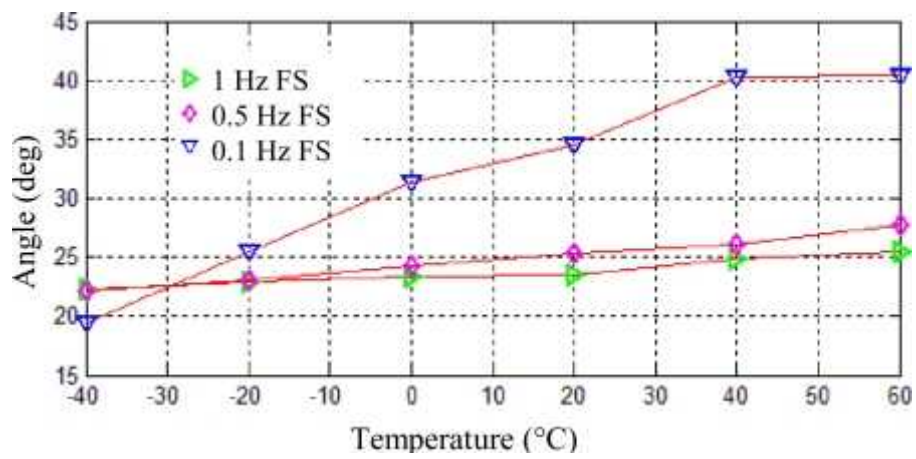
0,1 , 0,5 1 .  
4,

-40 °C 60 °C,

.2.20.

0,1 , 0,5 1 ,

20,27° , 5,58° 3,23°



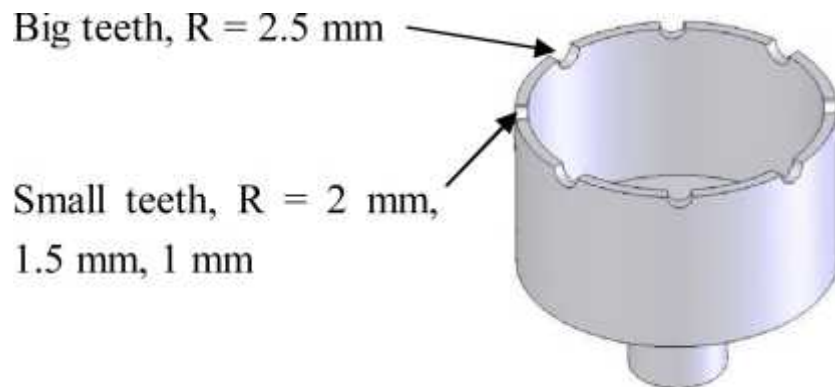
2.20.



2,5 ,  
 2 , 1,5 , 1 ,  
 0,5 , 1 1,5 ,

0,1

.2.21.



2.21.

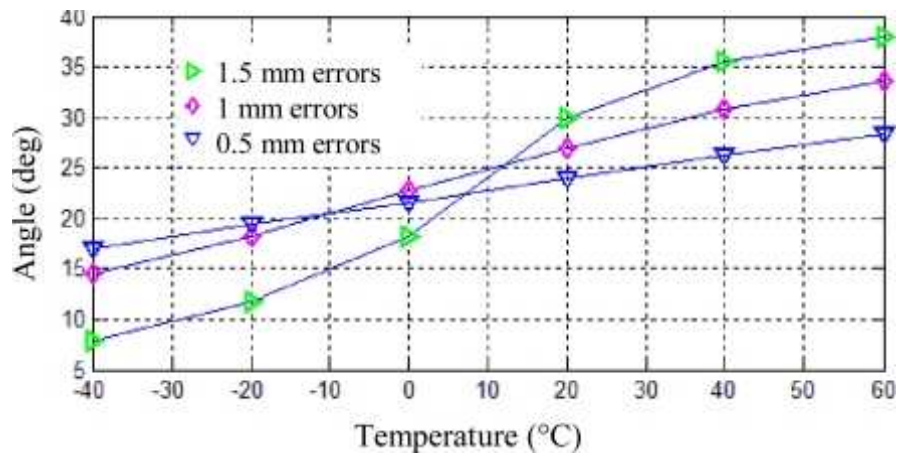
-40 °C 60 °C,  
 0,5 , 1 1,5 ,  
 . 2.22,

.2.22.

11,34°, 19,11°

30,09°

11,34° 30,09°.



2.22.

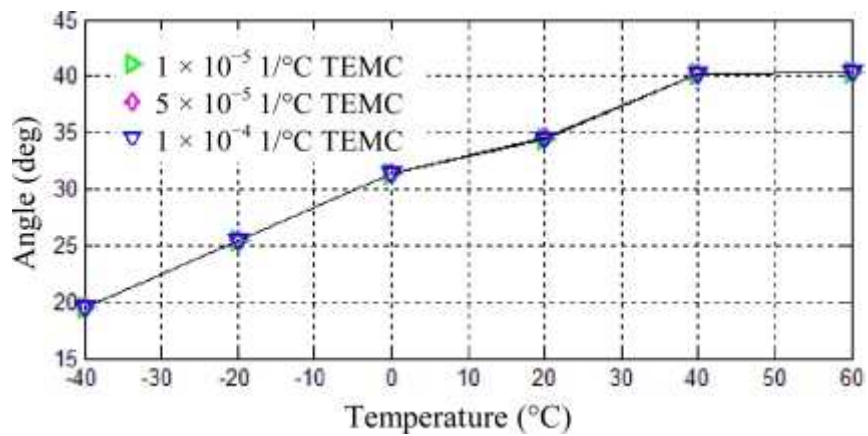
$10^{-4} \text{ 1/}^\circ\text{C}$ ,

$1 \times 10^{-5} \text{ 1/}^\circ\text{C}$ ,  $5 \times 10^{-5} \text{ 1/}^\circ\text{C}$   $1 \times$

0,1

$-40 \text{ }^\circ\text{C}$   $60 \text{ }^\circ\text{C}$

.2.23.



2.23.

$1 \times 10^{-4} \text{ 1/}^\circ\text{C}$ .

$1 \times 10^{-5} \text{ 1/}^\circ\text{C}$

$1 \times 10^{-5} \text{ 1/}^\circ\text{C}$

0,1

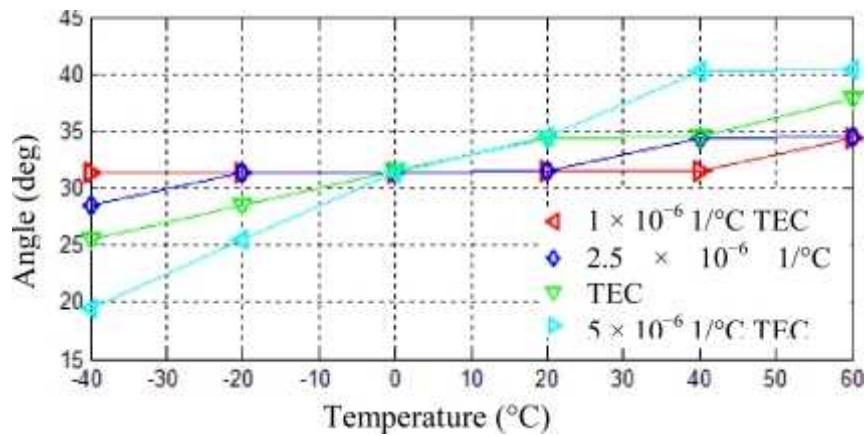
$1 \times 10^{-6} \text{ 1/}^\circ\text{C}$ ,  $2,5 \times 10^{-6} \text{ 1/}^\circ\text{C}$ ,  $5 \times 10^{-6} \text{ 1/}^\circ\text{C}$

-40 °C 60 °C

.2.24.

$1 \times 10^{-6} \text{ 1/}^\circ\text{C}$ ,  $2,5 \times 10^{-6} \text{ 1/}^\circ\text{C}$ ,  $5 \times 10^{-6} \text{ 1/}^\circ\text{C}$   $1 \times 10^{-5} \text{ 1/}^\circ\text{C}$ ,

2,98 °, 5,98°, 12,31° 20,87°



2.24.

.2.24,

2,98°

20,87°.

,

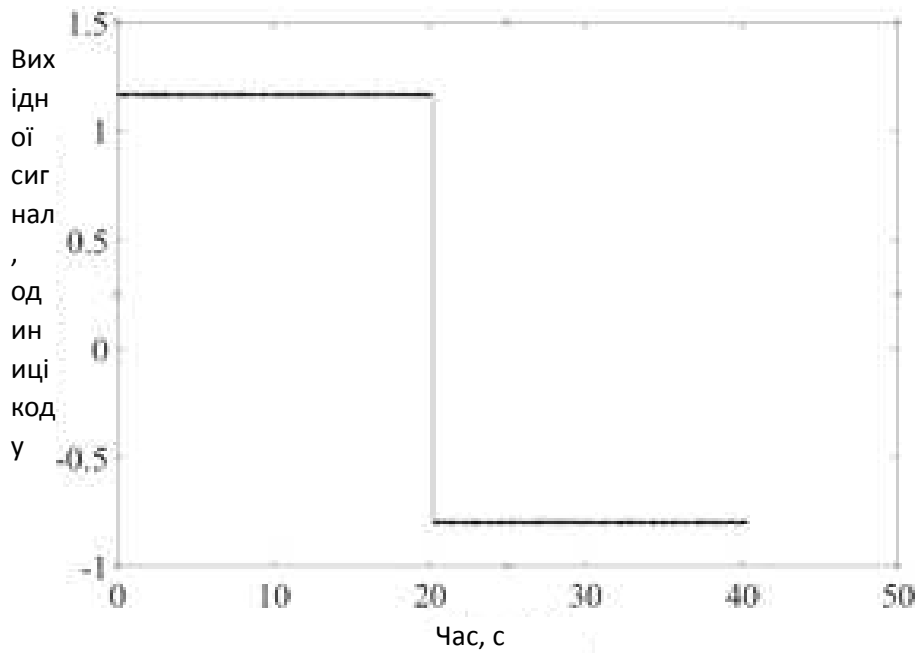
.

.



### 3.1.

Вихідний сигнал, одиначі код у / . =0 =60



. 3.1.  
500

. 3.1.

, . 3.1,

:

$$(\theta) = \frac{\bar{U}^+(\theta) - \bar{U}^-(\theta)}{2\Omega}; \quad \bar{U}^\pm(\theta) = \frac{1}{n} \sum_{i=1}^n U_i^\pm(\theta);$$

$$B(\theta) = \frac{\bar{U}^+(\theta) + \bar{U}^-(\theta)}{2} \#(3.1)$$

( ) -

;  $U_i^\pm(\theta)$  -

i-

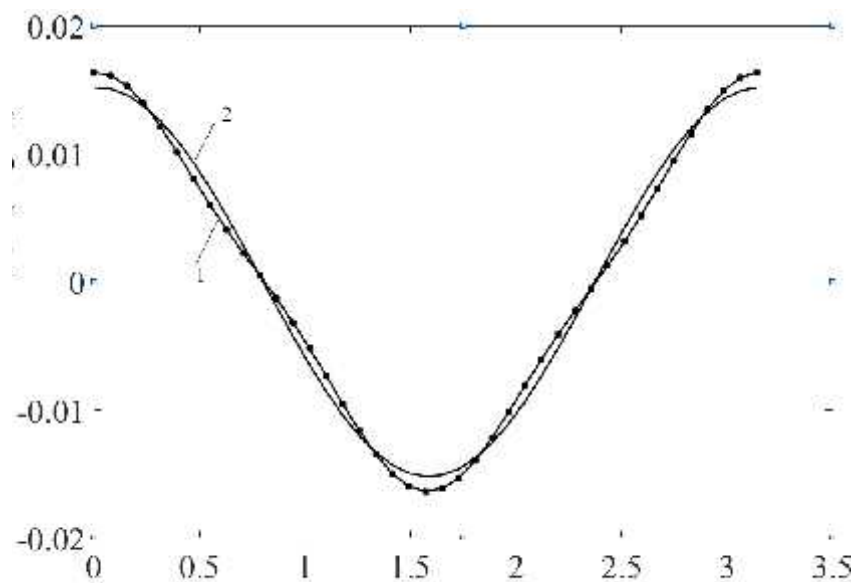
; n -

;  $B(\theta)$  -

=9

. 3.2

( 1)

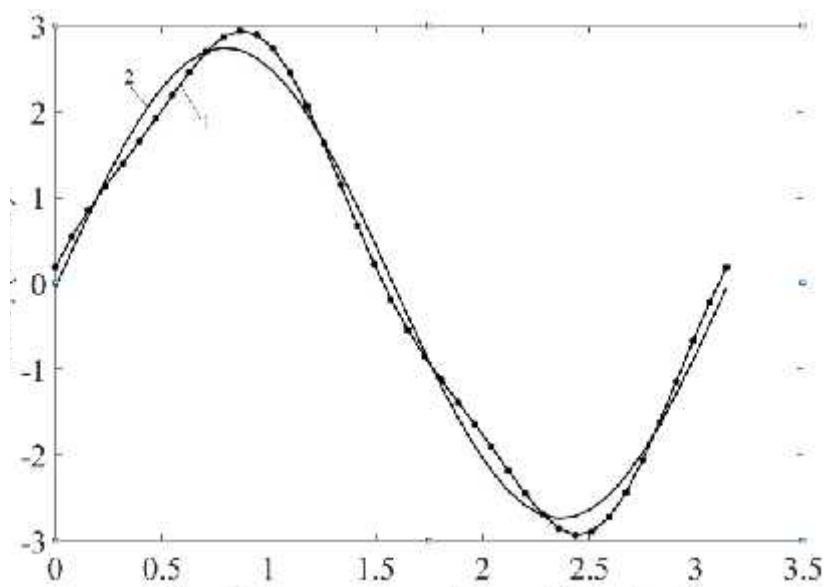


. 3.2,

,  
,  
( 2) 0.00091  
1/( / ). , 0,  
0,01640 1/( / ). = /4,

. 3.3

2 . 3.3





0,1925

20

B(0)=0.186

(0)=0.0164 1/( / ),

B(0)=0.186/0.0164=11.34 / .

### 3.2.

. 3.3,

=0

x<<1,

sin(x) | x

. 3.4.

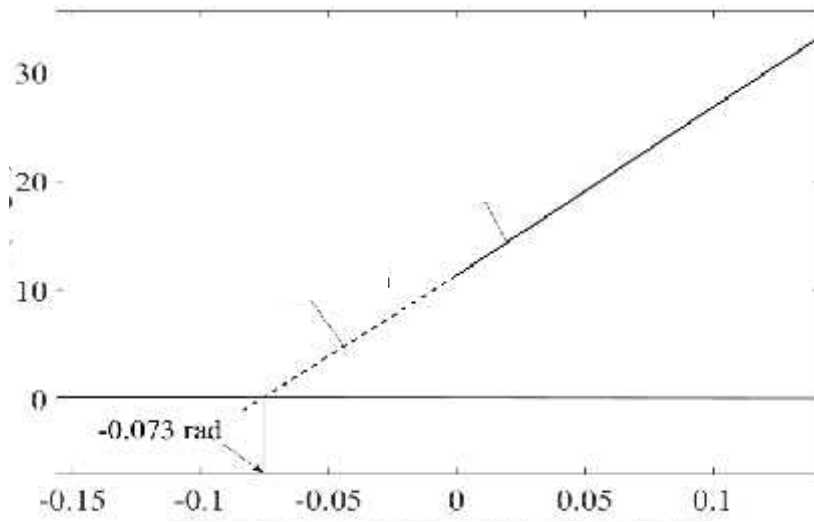
\*] -0.073

] -4.1826

\*] -

4.1826

0,01631



. 3.5 \* 0

1

/

0.006524 / .

- 0,0041 / . ,

. 3.5, . (3.1)

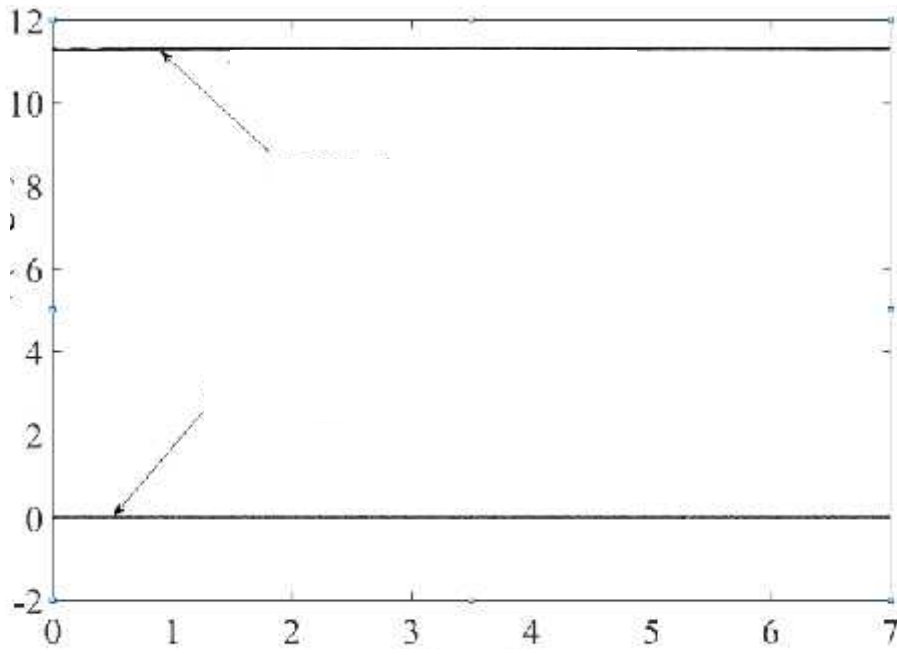
,

0.0032 / ,

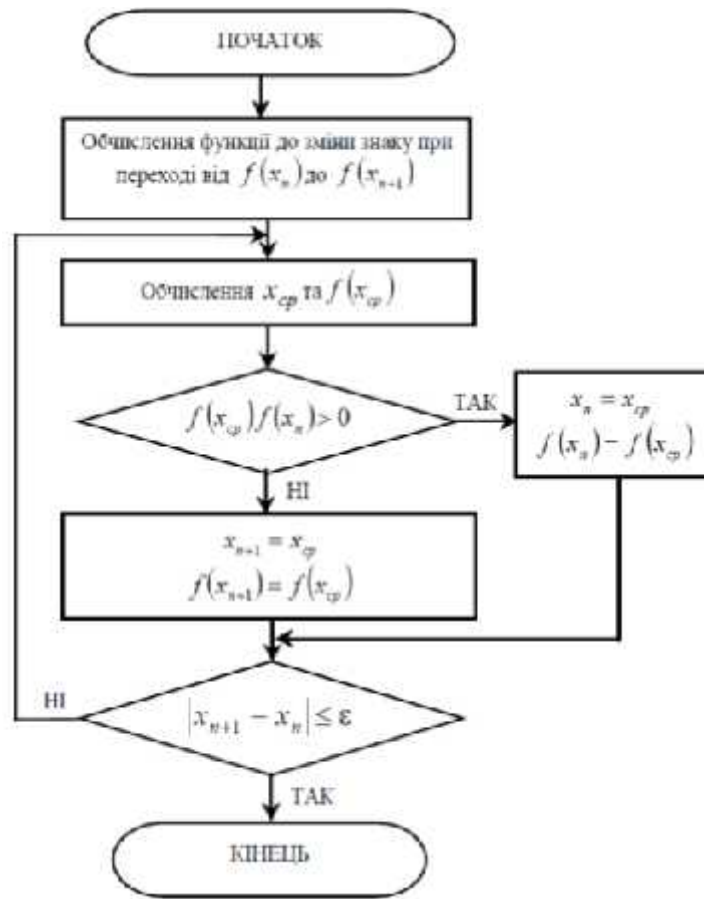
. 3.5 :

$$B( *) = 0.006524 - 0.00320.0033 /$$

$$B(0)/B(-0.073) \approx 3.4 \cdot 10^3$$

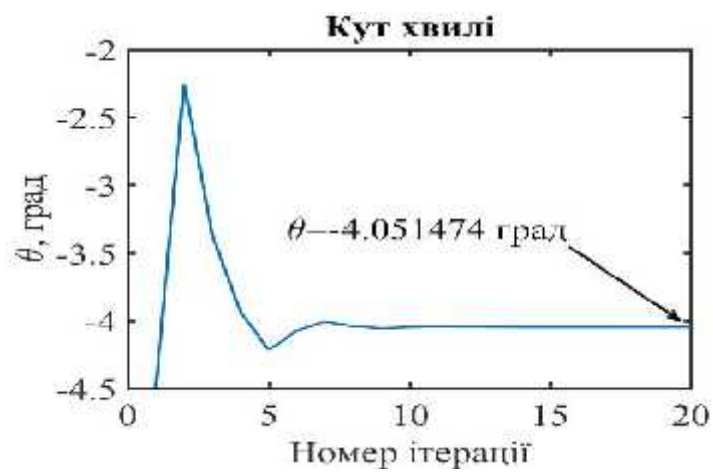


. 3.6.

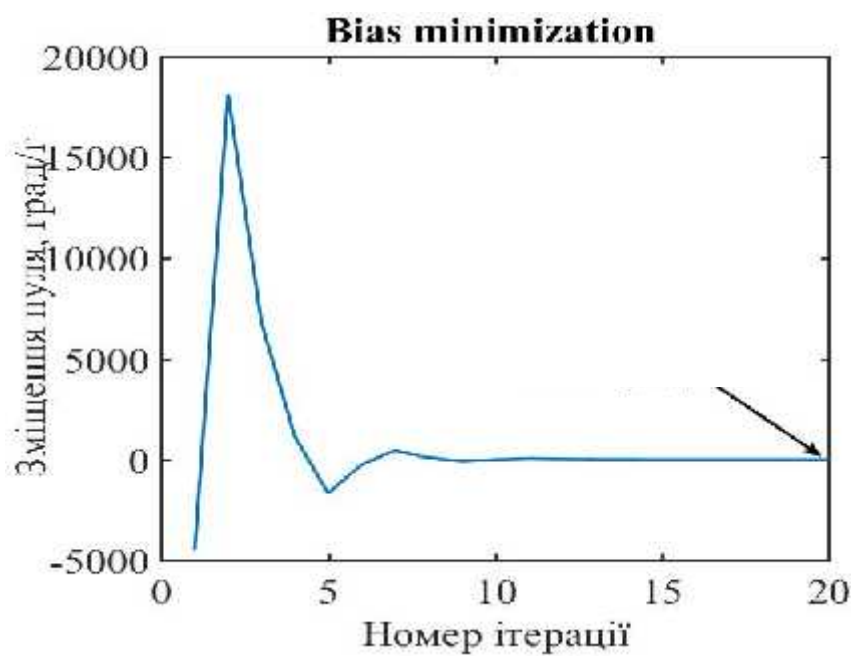


. 3.7

( ) 0



. 3.8



, 20

0.08 / .

/2.

\*

20

0.08 / ,



## 4.2.

( )

:

,

,

,

,

,

,

,

,

—

,

,

·

( , ),

·

—

,

,

,

,

,

,

,

·

—

,

« »

,

,

·

:

— ( , );

— ( , );

— ( )

).

30-40









,

,

.

,

,

,

.

.

:

— ;

— ;

— — ;

— ,

— ;

— ;

— :

— ( ‘ , )

— , , ;

— , , ( . ) —

— ;



5%

0,5 / <sup>2</sup>.

6-30 .

:

- 22-27 ;

- 6-12 ;

- 2-12 ;

- , 2-8 ;

- 8-27 ;

- 4-27 ;

- 4-14 ;

- 4-12 .

:

- , ;

- - , ,

, ;

- ,

, .

, ,

12.1. 012-90:

$L_u$

$L_v$ :

$L_a$

$$L_a = L_v + 20 \lg f - 60;$$

$$L_u = L_v - 20 \lg f + 60$$

Z  $u_0 = 8 \cdot 10^{-1}$  ;

Z  $v_0 = 5 \cdot 10^{-8}$  / ;

Z  $a_0 = 3 \cdot 10^{-4}$  /  $^2$ .

$v_0$

(  $a_0 = 2 \cdot 10^{-5}$  /  $^2$ ).

12.1. 012-90

( )

( )

$v,$

$1/3$

### 4.3.

.

,

:

—

;

—

,

;

—

,

;

—

—

,

,

,

;

—

.

,

.

,

,

,

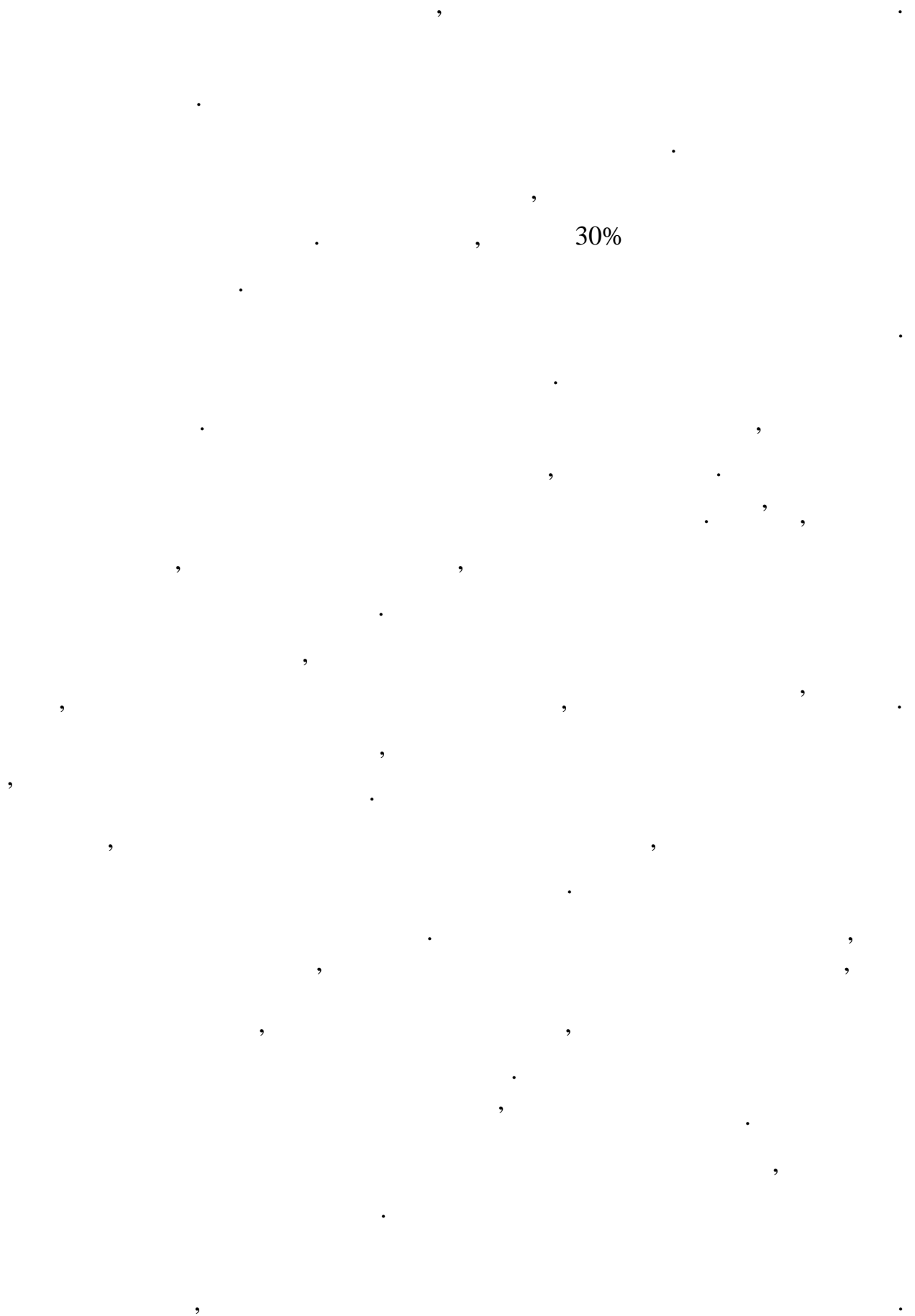
.

,



50%.

60%.



(

)

003-86.

,

.

.

,

(63-8000

,

,

.

,

,

.

,

.

,

.

.

.

.

,

,

,

,

,

.

LB, ,

—

63, 125, 250, 500, 1000, 2000, 4000, 8000 .

,

.

—

.

.

—

,

,

,

， ’ — .  
，  
，  
，  
30 12-15 ，  
3-4 .  
15-20%，  
8-12 .  
— ，  
， ，  
： ，  
100  
20-30 ， ，  
8 .  
30  
( — 2 ) .  
—  
" " .  
， ，  
，  
55 45 .  
80 .  
，  
，

4.

0.08 / .

. 20

1. Turner, G. History of Gyroscopes. 2004. Available online: <http://www.gyroscopes.org/history.asp> (accessed on 1 August 2022).
2. Tazartes, D. (Ed.) An historical perspective on inertial navigation systems. In Proceedings of the 2014 International Symposium on Inertial Sensors and Systems (ISISS), Laguna Beach, CA, USA, 25–26 February 2014; IEEE: Piscataway, NJ, USA, 2014.
3. Bergh, R.; Lefevre, H.; Shaw, H. An overview of fiber-optic gyroscopes. *J. Lightwave Technol.* 1984, 2, 91–107.
4. Seeger, J.; Lim, M.; Nasiri, S. (Eds.) *Development of High-Performance High-Volume Consumer Gyroscopes*; Solid-State Sensors, Actuators, and Microsystems Workshop: Hilton Head Island, SC, USA, 2010.
5. Mohammed, Z.; Gill, W.; Rasras, M. Modelling optimization and characterization of inertial sensors. In *Nanoscale Semiconductor Devices, and Sensors: Outlook and Challenges*; Springer: Berlin/Heidelberg, Germany, 2017.
6. De Groote, F.; Vandevyvere, S.; Vanhevel, F.; Orban de Xivry, J.-J. Validation of a smartphone embedded inertial measurement unit for measuring postural stability in older adults. *Gait Posture* 2021, 84, 17–23.
7. Mohammed, Z.; Gill, W.A.; Rasras, M.J.I.S.L. Double-comb-finger design to eliminate cross-axis sensitivity in a dual-axis accelerometer. *IEEE Sens. Lett.* 2017, 1, 1–4.
8. Ren, D.; Yan, M.; You, Z.J.T.; Technologies, M. Principle and research progress of resonant magnetometer. *Transducer Microsyst. Technol.* 2007, 26, 10–12.
9. Wendel, J.; Meister, O.; Schlaile, C.; Trommer, G.F. An integrated GPS/ -IMU navigation system for an autonomous helicopter. *Aerosp. Sci. Technol.* 2006, 10, 527–533.
10. Gaura, E.; Newman, R. *Smart and Sensor Systems*; World Scientific: Singapore, 2006.



11. Korvink, J.; Paul, O. : *A Practical Guide of Design, Analysis, and Applications*; Springer Science & Business Media: Berlin/Heidelberg, Germany, 2010.
12. Younis, M.I. *Linear and Nonlinear Statics and Dynamics*; Springer Science & Business Media: Berlin/Heidelberg, Germany, 2011.
13. Acar, C.; Shkel, A. *Vibratory Gyroscopes: Structural Approaches to Improve Robustness*; Springer Science & Business Media: Berlin/Heidelberg, Germany, 2008.
14. Acar, C.; Shkel, A.; Costlow, L.; Madni, A. Inherently Robust Micromachined Gyroscopes with 2-DOF Sense-Mode Oscillator. *J. Microelectromech. Syst.* 2006, *15*, 380–387.
15. Acar, C.; Shkel, A. An approach for increasing drive-mode bandwidth of vibratory gyroscopes. *J. Microelectromech. Syst.* 2005, *14*, 520–528.
16. Dong, L.; Avanesian, D. Drive-Mode Control for Vibrational Gyroscopes. *IEEE Trans. Ind. Electron.* 2008, *56*, 956–963.
17. Acar, C.; Schofield, A.R.; Trusov, A.A.; Costlow, L.E.; Shkel, A.M. Environmentally robust vibratory gyroscopes for auto-motive applications. *IEEE Sens. J.* 2009, *9*, 1895–1906.
18. Ghisi, A.; Mariani, S. Effect of Imperfections Due to Material Heterogeneity on the Offset of Polysilicon Structures. *Sensors* 2019, *19*, 3256.
19. Ma, Z.; Chen, X.; Jin, X.; Jin, Y.; Zheng, X.; Jin, Z. Effects of Structural Dimension Variation on the Vibration of Ring-Based Gyroscopes. *Micromachines* 2021, *12*, 1483.
20. Behera, A.R.; Shaik, H.; Rao, G.M.; Pratap, R. A Technique for Estimation of Residual Stress and Young's Modulus of Compressively Stressed Thin Films Using Microfabricated Beams. *J. Microelectromech. Syst.* 2019, *28*, 1039–1054.

21. Passaro, V.M.N.; Cuccovillo, A.; Vaiani, L.; De Carlo, M.; Campanella, C.E. Gyroscope Technology and Applications: A Review in the Industrial Perspective. *Sensors* 2017, *17*, 2284.
22. Liu, K.; Zhang, W.; Chen, W.; Li, K.; Dai, F.; Cui, F.; Wu, X.; Ma, G.; Xiao, Q. The development of micro-gyroscope technology. *J. Micromechanics Microeng.* 2009, *19*, 113001.
23. Pistorio, F.; Saleem, M.M.; Somà, A. A Dual-Mass Resonant Gyroscope Design with Electrostatic Tuning for Frequency Mismatch Compensation. *Appl. Sci.* 2021, *11*, 1129.
24. Nguyen, N.M.; Chang, C.-Y.; Pillai, G.; Li, S.-S. Design of piezoelectric bulk acoustic wave mode-matched gyroscopes based on support transducer. In Proceedings of the 2021 IEEE 34th International Conference on Micro Electro Mechanical Systems ( ), Gainesville, FL, USA, 25–29 January 2021.
25. Iga, Y.; Kanda, K.; Fujita, T.; Higuchi, K.; Maenaka, K. A design and fabrication of gyroscope using PZT thin films. In Proceedings of the 2010 World Automation Congress, Kobe, Japan, 19–23 September 2010.
26. Yeh, C.; Tsai, J.; Shieh, R.; Tseng, F.; Li, C.; Su, Y. A vertically supported ring-type gyroscope utilizing electromagnetic actuation and sensing. In Proceedings of the 2008 IEEE International Conference on Electron Devices and Solid-State Circuits, Hong Kong, China, 8–10 December 2008.
27. Saqib, M.; Mubasher Saleem, M.; Mazhar, N.; Awan, S.U.; Shahbaz Khan, U. Design and analysis of a high-gain and robust multi-DOF electro-thermally actuated gyroscope. *Micromachines* 2018, *9*, 577.
28. Senkal, D.; Efimovskaya, A.; Shkel, A.M. Minimal realization of dynamically balanced lumped mass WA gyroscope: Dual Foucault pendulum. In Proceedings of the 2015 IEEE International Symposium on Inertial Sensors and Systems (ISISS), Hapuna Beach, HI, USA, 23–26 March 2015.
29. Zhanshe, G.; Fucheng, C.; Boyu, L.; Le, C.; Chao, L.; Ke, S. Research development of silicon gyroscopes: A review. *Microsyst. Technol.* 2015, *21*, 2053–2066.

30. Armenise, M.N.; Ciminelli, C.; Dell'Olio, F.; Passaro, V.M. *Advances in Gyroscope Technologies*; Springer Science & Business Media: Berlin/Heidelberg, Germany, 2010.
31. Boxenhorn, B.; Greiff, P. A vibratory micromechanical gyroscope. *Guid. Navig. Control. Conf.* 1988.
32. Greiff, P.; Boxenhorn, B.; King, T.; Niles, L. Silicon monolithic micromechanical gyroscope. In Proceedings of the TRANSDUCERS'91: 1991 International Conference on Solid-State Sensors and Actuators Digest of Technical Papers, San Francisco, CA, USA, 24–27 June 1991.
33. Greiff, P.; Antkowiak, B.; Campbell, J.; Petrovich, A. Vibrating wheel micromechanical gyro. In Proceedings of the Position, Location and Navigation Symposium-PLANS'96, Atlanta, GA, USA, 22–25 April 1996.
34. Bernstein, J.; Cho, S.; King, A.; Kourepenis, A.; Maciel, P.; Weinberg, M. A micromachined comb-drive tuning fork rate gyroscope. In Proceedings of the IEEE Micro Electro Mechanical Systems, Fort Lauderdale, FL, USA, 10 February 1993.
35. Geiger, W.; Folkmer, B.; Merz, J.; Sandmaier, H.; Lang, W. A new silicon rate gyroscope. *Sens. Actuators A Phys.* 1999, *73*, 45–51.
36. Maenaka, K.; Ioku, S.; Sawai, N.; Fujita, T.; Takayama, Y. Design, fabrication and operation of                      gimbal gyroscope. *Sens. Actuators A Phys.* 2005, *121*, 6–15.
37. Jain, A.; Shekhar, C.; Gopal, R. Fabrication of two-gimbal Ni–Fe torsional micro-gyroscope by SU-8 based UV-LIGA process. *Microsyst. Technol.* 2014, *21*, 1479–1487.
38. Lee, J.S.; An, B.H.; Mansouri, M.; Al Yassi, H.; Taha, I.; Gill, W.A.; Choi, D.S.                      vibrating wheel on gimbal gyroscope with high scale factor. *Microsyst. Technol.* 2019, *25*, 4645–4650
39. Van Vu, T.; Tran, D.Q.; Chu, T.D. Matching mechanical response for a vibratory tuning fork gyroscope. *Microsyst. Technol.* 2020, *26*, 3865–3874. [

40. Dong, X.; Huang, Q.; Yang, S.; Huang, Y.; En, Y. Model and experiment of scale factor acceleration sensitivity of gyroscope in high acceleration environment. *Microsyst. Technol.* 2018, *25*, 3097–3103.
41. Che, L.; Xiong, B.; Li, Y.; Wang, Y. A novel electrostatic-driven tuning fork micromachined gyroscope with a bar structure operating at atmospheric pressure. *J. Micromech. Microeng.* 2009, *20*, 015025.
42. Sharma, A.; Zaman, F.; Amini, B.; Ayazi, F. A high-Q in-plane SOI tuning fork gyroscope. In Proceedings of the SENSORS, Vienna, Austria, 24–27 October 2004; pp. 467–470.
43. Nguyen, M.N.; Ha, N.S.; Nguyen, L.Q.; Chu, H.M.; Vu, H.N. Z-axis micromachined tuning fork gyroscope with low air damping. *Micromachines* 2017, *8*, 42.
44. Guan, Y.; Gao, S.; Jin, L.; Cao, L. Design and vibration sensitivity of a tuning fork gyroscope with anchored coupling mechanism. *Microsyst. Technol.* 2015, *22*, 247–254.
45. Guan, Y.; Gao, S.; Liu, H.; Jin, L.; Niu, S. Design and Vibration Sensitivity Analysis of a Tuning Fork Gyroscope with an Anchored Diamond Coupling Mechanism. *Sensors* 2016, *16*, 468.
46. Trusov, A.A.; Prikhodko, I.P.; Zotov, S.A.; Schofield, A.R.; Shkel, A.M. Ultra-high Q silicon gyroscopes with interchangeable rate and whole angle modes of operation. In Proceedings of the SENSORS, Waikoloa, HI, USA, 1–4 November 2010; pp. 864–867.
47. Xia, D.; Yu, C.; Kong, L. The Development of Micromachined Gyroscope Structure and Circuitry Technology. *Sensors* 2014, *14*, 1394–1473.
48. Putty, M.W.; Eddy, D.S. Microstructure for Vibratory Gyroscope. U.S. Patent 5,450,751, 19 September 1995.
49. Ayazi, F.; Najafi, K. Design and fabrication of high-performance polysilicon vibrating ring gyroscope. In Proceedings of the IEEE Eleventh Annual International Workshop on Micro Electro Mechanical Systems An Investigation of

Micro Structures, Sensors, Actuators, Machines and Systems, Heidelberg, Germany, 25–29 January 1998.

50. Ayazi, F.; Najafi, K. A HARPSS polysilicon vibrating ring gyroscope. *J. Microelectromech. Syst.* 2001, *10*, 169–179.

51. Ayazi, F.; Chen, H.; Kocer, F.; He, G.; Najafi, K. A High Aspect-Ratio Polysilicon Vibrating Ring Gyroscope. In Proceedings of the Solid-State Sensor Actuator Workshop, Hilton Head Island, SC, USA, 4–8 June 2000; Volume 10, pp. 4–8.

52. Guohong, H.; Najafi, K. A Single-Crystal Silicon Vibrating Ring Gyroscope. In Proceedings of the Technical Digest 2002 IEEE International Conference Fifteenth IEEE International Conference on Micro Electro Mechanical Systems, Las Vegas, NV, USA, 24 January 2002.

53. Kou, Z.; Liu, J.; Cao, H.; Shi, Y.; Ren, J.; Zhang, Y. A novel S-springs vibrating ring gyroscope with atmosphere package. *AIP Adv.* 2017, *7*, 125301.

54. Kou, Z.; Cui, X.; Cao, H.; Li, B. Analysis and Study of a Vibrating Ring Gyroscope with High Sensitivity. In Proceedings of the 2020 IEEE 5th Information Technology and Mechatronics Engineering Conference (ITOEC), Chongqing, China, 12–14 June 2020.

55. Syed, W.U.; An, B.H.; Gill, W.A.; Saeed, N.; Al-Shaibah, M.S.; Al Dahmani, S.; Choi, D.S.; Elfadel, I.A.M. Sensor Design Migration: The Case of a VRG. *IEEE Sens. J.* 2019, *19*, 10336–10346.

56. Cao, H.; Liu, Y.; Kou, Z.; Zhang, Y.; Shao, X.; Gao, J.; Huang, K.; Shi, Y.; Tang, J.; Shen, C.; et al. Design, Fabrication and Experiment of Double U-Beam Vibration Ring Gyroscope. *Micromachines* 2019, *10*, 186.

57. Gill, W.A.; Ali, D.; An, B.H.; Syed, W.U.; Saeed, N.; Al-Shaibah, M.; Elfadel, I.M.; Al Dahmani, S.; Choi, D.S. multi-vibrating ring gyroscope for space applications. *Microsyst. Technol.* 2020, *26*, 2527–2533.

58. Liang, F.; Liang, D.-D.; Qian, Y.-J. Dynamical analysis of an improved ring gyroscope encircled by piezoelectric film. *Int. J. Mech. Sci.* 2020, *187*, 105915.
59. Liang, F.; Liang, D.-D.; Qian, Y.-J. Nonlinear Performance of Vibratory Ring Gyroscope. *Acta Mech. Solida Sin.* 2020, *34*, 65–78.
60. Fujita, T.; Mizuno, T.; Kenny, R.; Maenaka, K.; Maeda, M. Two-dimensional micromachined gyroscope. In Proceedings of the International Solid State Sensors and Actuators Conference (Transducers' 97), Chicago, IL, USA, 19 June 1997.
61. Juneau, T.; Pisano, A.; Smith, J.H. Dual axis operation of a micromachined rate gyroscope. In Proceedings of the International Solid State Sensors and Actuators Conference (Transducers' 97), Chicago, IL, USA, 19 June 1997.
62. Tang, T.K.; Gutierrez, R.C.; Stell, C.B.; Vorperian, V.; Arakaki, G.A.; Rice, J.T.; Li, W.J.; Chakraborty, I.; Shcheglov, K.; Wilcox, J.Z.; et al. A packaged silicon vibratory gyroscope for microspacecraft. In Proceedings of the IEEE The Tenth Annual International Workshop on Micro Electro Mechanical Systems An Investigation of Micro Structures, Sensors, Actuators, Machines and Robots, Nagoya, Japan, 26–30 January 1997.
63. Kang, M.-S.; Youn, S.-K.; Cho, Y.-H.; Lee, K.B. Dynamic modeling of a tunable microgyroscope. *Sens. Mater.* 1998, *10*, 413–424.
64. Prikhodko, I.P.; Zotov, S.A.; Trusov, A.A.; Shkel, A.M. Foucault pendulum on a chip: Angle measuring silicon gyroscope. In Proceedings of the 2011 IEEE 24th International Conference on Micro Electro Mechanical Systems, Cancun, Mexico, 23–27 January 2011.
65. Prikhodko, I.P.; Zotov, S.A.; Trusov, A.A.; Shkel, A.M. Foucault pendulum on a chip: Rate integrating silicon gyroscope. *Sens. Actuators A Phys.* 2012, *177*, 67–78.

66. Zotov, S.A.; Trusov, A.A.; Shkel, A.M. High-Range Angular Rate Sensor Based on Mechanical Frequency Modulation. *J. Microelectromech. Syst.* 2012, *21*, 398–405.
67. Minotti, P.; Della, S.; Mussi, G.; Bonfanti, A.; Facchinetti, S.; Tocchio, A.; Zega, V.; Comi, C.; Lacaita, A.L.; Langfelder, G. High Scale-Factor Stability Frequency-Modulated Gyroscope: 3-Axis Sensor and Integrated Electronics Design. *IEEE Trans. Ind. Electron.* 2017, *65*, 5040–5050.
68. Xu, Q.; Hou, Z.; Kuang, Y.; Miao, T.; Ou, F.; Zhuo, M.; Xiao, D.; Wu, X. A Tuning Fork Gyroscope with a Polygon-Shaped Vibration Beam. *Micromachines* 2019, *10*, 813.
69. Xu, P.; Si, C.; He, Y.; Wei, Z.; Jia, L.; Han, G.; Ning, J.; Yang, F. A Novel High-Q Dual-Mass Tuning Fork Gyroscope Based on 3D Wafer-Level Packaging. *Sensors* 2021, *21*, 6428.
70. Khaled, A.; Salman, A.M.; Aljehani, N.S.; Alzahem, I.F.; Almikhlaifi, R.S.; Noor, R.M.; Seddiq, Y.M.; Alghamdi, M.S.; Soliman, M.; Mahmoud, M.A.E. An Electrostatic Roll-Pitch Rotation Rate Sensor with In-Plane Drive Mode. *Sensors* 2022, *22*, 702.
71. Taheri-Tehrani, P.; Izyumin, O.; Izyumin, I.; Ahn, C.H.; Ng, E.J.; Hong, V.A.; Yang, Y.; Kenny, T.W.; Boser, B.E.; Horsley, D.A. Disk resonator gyroscope with whole-angle mode operation. In Proceedings of the 2015 IEEE International Symposium on Inertial Sensors and Systems (ISISS), Hapuna Beach, HI, USA, 23–26 March 2015.
72. Senkal, D.; Ng, E.J.; Hong, V.; Yang, Y.; Ahn, C.H.; Kenny, T.W.; Shkel, A.M. Parametric drive of a toroidal rate integrating gyroscope demonstrating < 20 PPM scale factor stability. In Proceedings of the 2015 28th IEEE International Conference on Micro Electro Mechanical Systems ( ), Estoril, Portugal, 18–22 January 2015.
73. Khan, I.; Ting, D.S.K.; Ahamed, M.J. Design and development of a vibrating ring resonator with inner rose petal spring supports. *Microsyst. Technol.* 2020, *27*, 985–995.

74. Li, Z.; Gao, S.; Jin, L.; Liu, H.; Niu, S. Micromachined Vibrating Ring Gyroscope Architecture with High-Linearity, Low Quadrature Error and Improved Mode Ordering. *Sensors* 2020, *20*, 4327.
75. Tsai, D.-H.; Fang, W. Design and simulation of a dual-axis sensing decoupled vibratory wheel gyroscope. *Sens. Actuators A Phys.* 2006, *126*, 33–40.
76. Trusov, A.A.; Prikhodko, I.P.; Rozelle, D.; Meyer, A.; Shkel, A.M. 1 ppm precision self-calibration of scale factor in Coriolis vibratory gyroscopes. In Proceedings of the 2013 Transducers & Eurosensors XXVII: The 17th International Conference on Solid-State Sensors, Actuators and Microsystems (TRANSDUCERS & EUROSENSORS XXVII), Barcelona, Spain, 16–20 June 2013.
77. Din, H.; Iqbal, F.; Lee, B. Modelling and optimization of single drive 3-axis gyroscope. *Microsyst. Technol.* 2020, *26*, 2869–2877.
78. Li, C.; Yang, B.; Guo, X.; Chen, X. Design, Analysis and Simulation of a -Based Gyroscope with Differential Tunneling Magnetoresistance Sensing Structure. *Sensors* 2020, *20*, 4919.
79. R. Eley, C.H.J. Fox, S. McWilliam, CORIOLIS COUPLING EFFECTS ON THE VIBRATION OF ROTATING RINGS, *J Sound Vib*, 238(2000) 459-80.
80. V. Chikovani, Y.A. Yatsenko, A. Barabashov, P. Marusyk, E. Umakhanov, V. Taturin, Improved accuracy metallic resonator CVG, *Ieee Aero El Sys Mag*, 24(2009) 40-3.
81. V. Chikovani, O. Suschenko, Differential mode of operation for Coriolis vibratory gyro with ringlike resonator, *Electronics and Nanotechnology (ELNANO)*, 2014 IEEE 34th International Conference on, IEEE2014, pp. 451-5.
82. W.S. Watson, Vibratory gyro skewed pick-off and driver geometry, *Position Location and Navigation Symposium (PLANS)*, 2010 IEEE/ION, IEEE2010, pp. 171-9.
83. P.W. Loveday, C.A. Rogers, THE INFLUENCE OF CONTROL SYSTEM DESIGN ON THE PERFORMANCE OF VIBRATORY GYROSCOPES, *J Sound Vib*, 255(2002) 417-32.



84. S.K. Hong, Compensation of nonlinear thermal bias drift of Resonant Rate Sensor using fuzzy logic, *Sensors and Actuators A: Physical*, 78(1999) 143-8.
85. Y. Hsu, P. Chou, Y. Kuo, Drift Modeling and Compensation for Coriolis-Based Gyroscope Using a Wiener-Type Recurrent Neural Network, *IEEE Inertial Sensors*, Kauai, Hawaii, USA, 2017, pp. 39-42.
86. E.E. Aktakka, J.-K. Woo, K. Najafi, On-Chip Characterization of Scale-Factor of a Ring Gyroscope via a Micro Calibration Platform, *IEEE Inertial Sensors*, Kauai, Hawaii, USA, 2017, pp. 31-4.
87. F. Pellicano, M. Amabili, M.P. Paidoussis, Effect of the geometry on the non-linear vibration of circular cylindrical shells, *Int J Nonlinear Mech*, 37(2002) 1181-98.
88. Y.G. Martynenko, I.V. Merkuriev, V.V. Podalkov, Dynamics of a ring micromechanical gyroscope in the forced-oscillation mode, *Gyroscopy and Navigation*, 1(2010) 43-51.
89. Y. Liu, F. Chu, Nonlinear vibrations of rotating thin circular cylindrical shell, *Nonlinear Dynam*, 67(2012) 1467-79.
90. C. Jihyun, A. Samuel, Nonlinear Dynamic Response of Ring-Based Vibratory Angular Rate Sensors, 50th AIAA/ASME/ASCE/AHS/ASC Structures, Structural Dynamics, and Materials Conference, American Institute of Aeronautics and Astronautics 2009.
91. D. Kristiansen, O. Egeland, Nonlinear Oscillations in Coriolis-Based Gyroscopes, *Nonlinear Dynam*, 19(1999) 193-235.
92. Y. Zhang, X. Wu, Y. Wu, X. Xi, Y. Tao, Nodal vibration and pattern angle error analysis of the imperfect resonators for vibratory cylinder gyroscopes, *International Journal of Precision Engineering and Manufacturing*, 17(2016) 419-26.
93. X. Xi, Y. Wu, X. Wu, Y. Tao, X. Wu, Investigation on standing wave vibration of the imperfect resonant shell for cylindrical gyro, *Sensors and Actuators A: Physical*, 179(2012) 70-7.
94. M.I. Younis, *Linear and Nonlinear Statics and Dynamics*, 1 ed., US: Springer 2011.

95. W. Thomson, *Theory of Vibration with Applications*: Taylor & Francis; 1996.
96. D.D. Lynch, Coriolis Vibratory Gyros, In *Proceedings of Symposium Gyro Technology*, Stuttgart, Germany, 1998.
97. K. Rourke, S. McWilliam, C.H.J. Fox, MULTI-MODE TRIMMING OF IMPERFECT RINGS, *J Sound Vib*, 248(2001) 695-724.
98. Y. Tao, X. Xi, D. Xiao, Y. Tan, H. Cui, X. Wu, Precision balance method for cupped wave gyro based on cup-bottom trimming, *Chin J Mech Eng-En*, 25(2012) 63-70.
99. Yongmeng Zhang, Xuezhong Wu, Xiang Xi, Yu Xin, Jiangkun Sun, Yulie Wu, Analysis and experiment of the zero bias drift of the vibratory cylinder gyroscope caused by nonlinear vibration, *Sensors and Actuators A: Physical*, Volume 267, 2017, Pages 334-341
100. B. Junlong, C. Wenjie and C. Tao, "Compensation for gyroscope zero bias stability," *2013 Chinese Automation Congress*, Changsha, China, 2013, pp. 744-748
101. Matveev, V.A.; Basarab, M.A. *Solid State Wave Gyros*, 1st ed.; Yang, Y., Zhao H., Eds.; National Defense Industry Press: Beijing, China, 2007; pp. 31-35.
102. Wu, L.F.; Zhang, F.X. The study of the scale factor of micro-machined gyroscope. *IEICE Electron. Express* 2008, 5, 840-845.
103. Wu Y, Xi X, Tao Y, Wu X, Wu X. A study of the temperature characteristics of vibration mode axes for vibratory cylinder gyroscopes. *Sensors (Basel)*. 2011;11(8):7665-77.